

Re: Manuscript acp-2016-1100, "Global deposition of total reactive nitrogen oxides from 1996 to 2014 constrained with satellite observations of NO<sub>2</sub> columns" by Jeffrey A. Geddes and Randall V. Martin

Dear Handling Editor,

Please find attached our full response to the reviewer comments. We respond to each reviewer comment individually, followed by the relevant changes to our manuscript.

A full copy of our manuscript with tracked changes is included.

Thank you for your time and consideration of our manuscript.

Jeffrey A. Geddes

[jgeddes@bu.edu](mailto:jgeddes@bu.edu)

### Response to Referee #1

We thank the reviewer very much for their constructive comments. We respond to each comment individually below, followed by changes to the manuscript.

**Reviewer Comment:** My first comment is that the present manuscript is missing some description and explanation of the top-down NO<sub>x</sub> emissions. First, measurements from three satellite instruments are used to estimate the long-term NO<sub>x</sub> emissions. Are there any instrumental differences among the three satellite products? If so, how do you reconcile them?

**Author Response:** The referee makes a good point bringing up the instrumental differences between satellite products (a similar concern was raised by another reviewer). The most important differences are the overpass times and the horizontal footprint of individual observations. First, the GOME, SCIAMACHY, and GOME-2 overpass times are roughly 10:30 a.m., 10:00 a.m., and 9:30 a.m. respectively. Second, their horizontal footprints are roughly 320 km x 40 km, 60 km x 30 km, and 80 km x 40 km respectively. We reconciled these three records by consulting published literature and by closely examining the overlapping time periods ourselves, and concluded that a consistent time series is achieved without requiring additional corrections. The reason for this is largely because the daily satellite observations were all gridded to a regular coarse grid of 2° x 2.5° latitude by longitude. Using a comparison with long-term ground-based MAX-DOAS observations, Irie et al. (2012) demonstrated that there is no inherent biases in either SCIAMACHY or GOME-2 that would preclude their combination into a single record. The work of van der A (2008) and Konovalov et al. (2010) show that a self-consistent record can be achieved by downgrading the spatial footprint of the higher resolving instruments (e.g. through smoothing or convolution) to that of the lowest resolving instrument. This is what we have achieved by gridding all the observations to 2° x 2.5°. The combination of these observations is also aided by the fact that the retrieval algorithm for obtaining tropospheric NO<sub>2</sub> column density from all three instruments is the same (<http://www.temis.nl/airpollution/no2.html>).

We further examined our approach by inspecting the timeseries from individual 2° x 2.5° pixels over selected populated regions. These are shown in Figure D1.

Given the evidence from this figure, and consensus in the literature, we concluded that the instrumental differences between instruments are inconsequential to our analysis.

In response to the referee's comment, we have modified our manuscript to include the additional citations and to elaborate on our reasoning for combining the satellite instrument records despite their instrumental differences:

“We calculate top-down surface NO<sub>x</sub> emissions from 1996 to 2014 using observations from GOME (1995-2003), SCIAMACHY (2002-2011) and GOME-2 (2007- ). The similar overpass time of these three instruments (from about 9:30 a.m. to 10:30 a.m. local time) facilitates their combination to provide consistent long-term coverage (van der A et al., 2008; Konovalov et al. 2010; Geddes et al., 2016; Hilboll et al., 2013). We achieve consistency across all three instruments despite their varying pixel sizes (320 km x 40 km, 60 km x 30 km, and 80 km x 40 km for GOME, SCIAMACHY, and GOME-2 respectively) by gridding the daily observations from each to a regular coarse grid of 2° x 2.5° latitude by longitude.”

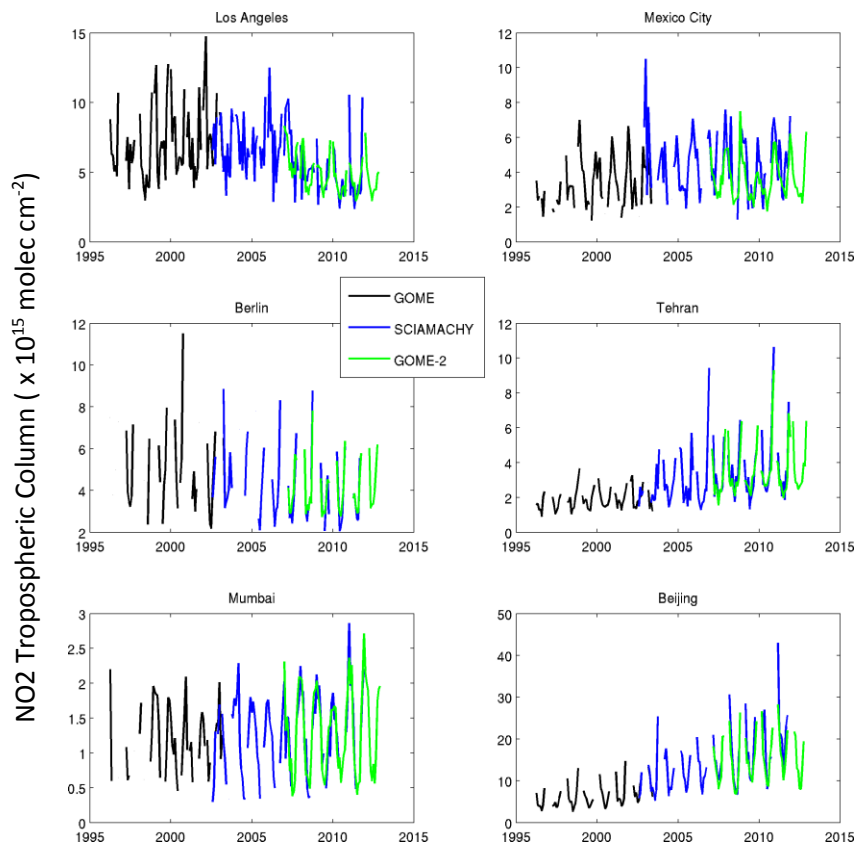


Figure D1: Monthly mean tropospheric NO<sub>2</sub> from GOME, SCIAMACHY, and GOME-2 showing consistent agreement during overlap between instruments.

**RC:** Second, the three satellite instruments have some overlapping time periods (e.g. 2007-2011 for SCIAMACHY and GOME-2). How do you use them for emission estimates during these periods? While these may have been presented in another study, a brief description here will help readers to better understand the method.

**AR:** In the case of GOME and SCIAMACHY, their period of overlap is small (June 2002 – April 2003). We use GOME observations alone for 2002, and SCIAMACHY observations alone for 2003. During the overlap between SCIAMACHY and GOME-2 (2007-2011), we use the GOME-2 observations given its more frequent global coverage (roughly every day) compared to SCIAMACHY (roughly every 6 days). We therefore use SCIAMACHY from years 2003-2006, and GOME-2 from years 2007-2014.

In response to the referee’s comment, we have added the following to our manuscript:

“In our study, we use GOME observations for years 1996 to 2002, SCIAMACHY observations for years 2003 to 2006, and GOME-2 observations for years 2007 to 2014”.

**RC:** And third, I strongly suggest present more information and analyses on the global top-down NO<sub>x</sub> emissions and their trends during the focused period by adding more text and a figure. This is not clear at present, and will be really helpful to understand the trends in NO<sub>y</sub> deposition as presented in Figure 6 and 7.

**AR:** We thank the referee for their suggestion, and agree that including details on the top-down emissions would be useful. We believe a table would be the optimal way to share this information. We have also included anthropogenic HNO<sub>3</sub> fluxes (from shipping emissions) to our calculation of total emissions to demonstrate full mass balance with NO<sub>y</sub> deposition.

In response to this comment, we have added the following material to our manuscript:

“Table 1 shows the annual global top-down NO<sub>x</sub> emissions from our calculations. We derive global mean satellite-constrained NO<sub>x</sub> emissions from 1996-2014 of  $55.6 \pm 3.4$  Tg N yr<sup>-1</sup>. Our top-down global NO<sub>x</sub> emissions for 2001 of 52.3 Tg N are consistent with the mean from over 20 models used in the Coordinated Model Studies Activities of the Task Force on Hemispheric Transport of Air Pollution (HTAP) for the same year of  $46.6 \pm 7.8$  Tg N (Vet et al. 2014).”

Table 1: Global top-down NO<sub>x</sub> emissions calculated using the finite mass balance inversion approach in combination with observations from GOME, SCIAMACHY, and GOME-2.

Year	Global NO <sub>x</sub> Emissions (Tg N yr <sup>-1</sup> ) <sup>a</sup>
1996	60.1
1997	58.4
1998	59.2
1999	59.6
2000	53.4
2001	52.3
2002	55.1
2003	50.1
2004	51.5
2005	51.2
2006	50.0
2007	54.7
2008	56.1
2009	55.9
2010	57.5
2011	58.9
2012	59.3
2013	58.5
2014	54.0
Mean	$55.6 \pm 3.4$

<sup>a</sup> Includes anthropogenic HNO<sub>3</sub> flux of  $2.3 \pm 0.1$  Tg N yr<sup>-1</sup>.

**RC:** Monthly mean simulated NO<sub>2</sub> columns are calculated using days with coincident satellite observations”. How do you select coincident days when using monthly-mean gridded satellite NO<sub>2</sub> observations (Line 11)? And how do you sample the model simulation? Please clarify.

**AR:** First, we grid the daily NO<sub>2</sub> tropospheric column retrievals to a regular 2° x 2.5° grid, then calculate monthly means ourselves. Therefore, we are able to keep track of which 2° x 2.5° grid boxes have satellite observations that pass quality control on each individual day. From our simulations we output late morning mean vertical NO<sub>2</sub> column profiles every day. Using this information, we calculate monthly mean tropospheric NO<sub>2</sub> columns from the model simulation only on days that are coincidentally sampled by successful satellite observations.

In response to the referee's comment, we have clarified this in our manuscript in the following places:

"We achieve consistency across all three instruments despite their varying pixel sizes (320 km x 40 km, 60 km x 30 km, and 80 km x 40 km for GOME, SCIAMACHY, and GOME-2 respectively) by gridding the daily observations from each to a regular coarse grid of 2° x 2.5° latitude by longitude."

"In all cases, monthly mean simulated NO<sub>2</sub> columns are calculated using days with coincident satellite observations. The simulated NO<sub>2</sub> vertical column is output daily for late morning."

**RC:** Do you mean you do not change the seasonality of NO<sub>x</sub> emissions in the model? Please clarify. And what is the NO<sub>x</sub> emission seasonality in the model? This is not described in the Appendix

**AR:** The referee is correct. We have not changed the seasonality of NO<sub>x</sub> emissions in the model. We assume that the scaling factor determined from coincidentally sampled model and satellite NO<sub>2</sub> tropospheric columns applies uniformly to the model prior emissions all year long regardless of whether successful satellite observations are available.

In response to the referee's comment, we have modified our manuscript to clarify our approach:

"In all cases, monthly mean simulated NO<sub>2</sub> columns are calculated using days with coincident satellite observations. The simulated NO<sub>2</sub> vertical column is output daily for late morning. We calculate scaling factors for every month with available satellite observations, then calculate an annual mean scaling factor that is used to infer annual mean from the mean monthly top-down emissions. Our top-down emissions retain the same seasonality as the prior emissions to mitigate concerns about seasonally missing data (such as from snow or monsoonal clouds)."

We have also added the following details regarding the emission seasonality to the Appendix:

"Monthly scaling of NO<sub>x</sub> emissions are included in North America (based on the VISTAS inventory), Europe (based on the EMEP inventory), and Asia (based on the Zhang et al. (2009) inventory). Monthly scaling of EDGAR emissions is based on the seasonality from the Global Emission Inventory Activity (Benkovitz et al 1996)."

**RC:** Is there any trends in the export efficiency or changes in the export fraction during the period 1996-2014 over the US and Asia? From Line 11 below, it appears that the export fractions over Europe have a decreasing trend.

**AR:** We thank the reviewer for their comment, and have evaluated the statistical significance of trends in export fraction over each region in the same manner as our evaluation of long term trends in deposition.

In response to the referee's comment, we have added the following details to our manuscript:

"We estimate a similar fraction of NO<sub>x</sub> export from the continental US using our observationally-constrained simulation (34% ± 2% from 1996-2014), with a small declining trend from a maximum of 38% in 1999 to a minimum of 31% in 2013.

"We calculate mean export of NO<sub>x</sub> emissions from western European countries to be 45% ± 4%, with a notable decreasing trend from a maximum of 50% in 1997 to a minimum of 39% in 2014."

"We estimate that an average of 24% ± 4% emissions from China are exported, varying over time from as little as 15% of emissions in 1998 to a maximum of 31% of emissions in 2011 (an overall increasing trend)."

**RC:** A recent study on atmospheric nitrogen deposition over China reported a NO<sub>y</sub> export fraction of 36% (Zhao et al., 2017), not that different from the values for Europe and the US, compared with 24% in this study. Can you explain why? different NO<sub>x</sub> emissions, inclusion of adjacent oceans, or model horizontal resolution?

**AR:** We thank the reviewer for this important reference, which we have added to our manuscript. In our opinion, the most obvious explanation for the discrepancy is in model resolution or perhaps the rapidly changing satellite-constrained emissions over this period of time, which peak in China in 2011.

In response to the referee's comment, we have made the following changes to our manuscript:

"We estimate that an average of 24% ± 4% emissions from China are exported, varying over time from as little as of 15% of emissions in 1998 to a maximum of 31% of emissions in 2011 (an overall increasing trend). Zhao et al. (2017) used a higher resolution (0.5° x 0.667°) GEOS-Chem simulation and estimated that 36% of China's NO<sub>x</sub> emissions over 2008-2012 are exported. We calculate an export fraction of around 27% for the same time period. The discrepancy between the two estimates may be attributed to the coarser horizontal resolution of our simulation (2° x 2.5°), pointing to important resolution-dependent effects in global simulations of deposition. Other factors may include the use of different NO<sub>x</sub> emissions (our satellite-constrained emissions indicate rapid change over this period of time), and the treatment of adjacent oceans."

**RC:** Please explain "perturbing NH<sub>3</sub> emissions everywhere". Increase or decrease? Do you change all anthropogenic and natural NH<sub>3</sub> emissions, including the oceanic NH<sub>3</sub> emissions?

**AR:** In response to the referee's comments, we have clarified the approach in our manuscript:

"Contemporary emissions of NH<sub>3</sub> are highly uncertain (Reis et al., 2009), so we perform a sensitivity experiment by perturbing (increasing) all anthropogenic and natural NH<sub>3</sub> emissions in the model by 25% for the year 2012."

**RC:** The unit "kg N ha<sup>-1</sup> yr<sup>-2</sup>" here might be confusing. Suggest add here "at a rate of..." or use annual deposition changes during the period.

**AR:** We thank the referee for their suggestion. In response, we have modified our manuscript to use the following wording:

“NO<sub>y</sub> deposition declined most steeply throughout the northeastern United States at a rate of up to -0.6 kg N ha<sup>-1</sup> yr<sup>-2</sup>”

“In Europe, statistically significant declines at a rate of up to -0.1 kg N ha<sup>-1</sup> yr<sup>-2</sup> are seen over some western countries.”

“On the other hand, NO<sub>y</sub> deposition has increased substantially throughout East Asia, exceeding a rate of +0.6 kg N ha<sup>-1</sup> yr<sup>-2</sup> in some parts.”

**RC:** Energy statistics are used to scale emissions between 1996 and 2010. How about emissions after 2010? Please clarify.

**AR:** We clarify this in our manuscript:

“For other species and for emissions beyond 2010, the closest available year is used.”

**RC:** Please state in the figure caption that the sensitivity test is for the year 2012.

**AR:** In response to the reviewer’s comment, we have added this to the figure caption.

#### **REFERENCES:**

Benkovits et al. (1996), Global gridded inventories of anthropogenic emissions of sulfur and nitrogen, *Journal of Geophysical Research-Atmospheres*, 101, 29239–29253

Irie et al. (2012), Quantitative bias estimates for tropospheric NO<sub>2</sub> columns retrieved from SCIAMACHY, OMI, and GOME-2 using a common standard for East Asia, *Atmospheric Measurement Techniques*, 5, 2403-2411

Konovalov et al. (2010) Multi-annual changes of NO<sub>x</sub> emissions in megacity regions: nonlinear trend analysis of satellite measurement based estimates, *Atmos. Chem. Phys.*, 10, 8481–8498

van der A et al. (2008), Trends, seasonal variability, and dominant NO<sub>x</sub> source derived from a ten year record of NO<sub>2</sub> measured from space, *Journal of Geophysical Research-Atmospheres*, 113, doi:10.1029/2007JD009021

Zhao et al. (2017), Atmospheric nitrogen deposition to China: A model analysis on nitrogen budget and critical load exceedance, *Atmospheric Environment*, 153, 32-40

## Response to Referee #2

We thank the reviewer very much for their constructive comments. We respond to each comment individually below, followed by changes to the manuscript.

**Reviewer Comment:** My major comment is that I recommend a coherent section on model and data uncertainties that may affect your analysis and conclusions. Here are some examples of what such a discussion may include:

MERRA meteorological fields: Are there any biases in precipitation or transport that may affect your results, such as through simulated wet deposition? Are there any known biases that change over time in MERRA, such as occur as new observations are brought into the assimilation system over your 20 year simulation period? These are important biases to discuss as global coverage of surface observations (e.g., wet deposition) are sparse over most of the globe.

GEOS-Chem: No model is perfect? Any known issues?

Chemistry: What are the known chemistry uncertainties in the relevant reaction mechanisms? You've answered this with your sensitivity test in Section 3.4.

Emissions: Are there biases? For instance, are the NEI NO<sub>x</sub> emissions biased?

**Author Response:** We agree with the referee that there could be a larger discussion on model and data uncertainties that may affect our analysis.

In response to the reviewer's comment, we have added the following discussion section to our manuscript:

### "3.5 Other Considerations

A number of other uncertainties are important in an inversion of satellite NO<sub>2</sub> columns to calculate surface NO<sub>x</sub> emissions and simulate of long-term NO<sub>y</sub> deposition. These can depend on, for example, the choice of inversion approach, errors in the satellite retrieval, and uncertainties in model processes (e.g. emissions, boundary layer mixing, chemical NO<sub>x</sub> sinks, meteorology, and dry deposition).

Cooper et al. (2017) found that the finite mass balance inversion approach used here can be improved upon by using an iterative method that performs with similar accuracy as a four-dimensional variational data assimilation. Multi-constituent data assimilation also shows considerable promise for constraints on surface NO<sub>x</sub> emissions (Myazaki et al. 2017). Satellite retrieval algorithms continue to develop with advances that will improve the accuracy of future estimates of satellite-constrained NO<sub>y</sub> deposition.

Uncertainties in model processes are also of interest. For example, uncertainties in the chemical sink of NO<sub>x</sub> alone (e.g. the rate of HNO<sub>3</sub> formation, heterogeneous loss of N<sub>2</sub>O<sub>5</sub> onto aerosol) can have a substantial impact on top-down emissions estimates (Stavrakou et al., 2013), suggesting more fundamental work in constraining these processes is required. Lin et al. (2010) found that top-down NO<sub>x</sub> emissions estimates over East Asia are sensitive to other model uncertainties including planetary boundary layer mixing scheme, lightning emissions, diurnal profile of emissions, and a-priori NO<sub>x</sub>, CO, and VOC emissions. Uncertainties in model meteorology are also important. For example, the MERRA precipitation fields used in our study are known to correlate weakly with observational datasets (Rienecker et al., 2011), but improvements can be expected from MERRA-2 due to the inclusion of



gauge- and satellite-based precipitation corrections (Reichle et al., 2017). Finally, dry deposition schemes are also highly variable among models (Flechard et al., 2011; Hardacre et al., 2015), and future work in dry deposition evaluation should be a priority.

Nonetheless, despite these uncertainties we find a high degree of consistency between observations and our predictions in the long-term changes to deposition. Evidence continues to emerge about potential biases in bottom-up inventories (e.g. Travis et al. 2016), and our observational constraint on NO<sub>x</sub> emissions mitigates against such biases. We expect continued advancements in inversion approaches, satellite retrieval algorithms, and fundamental atmospheric chemistry processes will allow for increasingly accurate satellite-based constraints on deposition.”

**RC:** Section 3.4: How does the model simulation of ammonia compare to observations, such as from AIRS, and the very long record of SO<sub>2</sub>, such as from the same instruments that you use for NO<sub>2</sub>

**AR:** The reviewer raises a good question. GEOS-Chem ammonia simulations have been explored by other groups (e.g. Schiferl et al. 2016), and suggest that the model can underestimate interannual variability and concentrations of ammonia. A new NH<sub>3</sub> emission inventory is now available (Paulot et al., 2014), but this inventory is still only representative of a short period of time (2005-2008), thus potentially introducing similar errors in other years of our analysis anyway. Our perturbation experiment with NH<sub>3</sub> emissions (Section 3.4) is an attempt to investigate the dependence of NO<sub>y</sub> deposition on NH<sub>3</sub> emission uncertainties. We found that reasonable uncertainties/changes in NH<sub>3</sub> emissions (~25%) are generally inconsequential to the spatial distribution of predicted NO<sub>y</sub> deposition over land. We did not feel the need to repeat such an experiment with SO<sub>2</sub> emissions, since SO<sub>2</sub> emissions tend to be less uncertain than NH<sub>3</sub> emissions and will therefore have even less of an impact on the predicted spatial distribution of NO<sub>y</sub> deposition. We argue that an evaluation of GEOS-Chem simulated NH<sub>3</sub> and SO<sub>2</sub> is thus beyond the scope of our study, and would not have substantial bearing on the conclusions in our manuscript.

**RC:** It is no easy task to create an inter-consistent long-term data record using multiple satellite observations, so this topic deserves some discussion. What are the uncertainties and potential biases? For example, a priori vertical profiles change over time

**AR:** We agree with the reviewer that creating a long-term record across multiple satellite records is not necessarily a trivial task (a similar concern was raised by another reviewer). In our case, we concluded that a consistent time series can be achieved without requiring additional corrections. The reason for this is largely because the daily satellite observations were all gridded to a regular coarse grid of 2° x 2.5° latitude by longitude. Using a comparison with long-term ground-based MAX-DOAS observations, Irie et al. (2012) demonstrated that there is no inherent biases in either SCIAMACHY or GOME-2 that would preclude their combination into a single record. The work of van der A (2008) and Konovalov et al. (2010) show that a self-consistent record can be achieved by downgrading the spatial footprint of the higher resolving instruments (e.g. through smoothing or convolution) to that of the lowest resolving instrument. This is what we have achieved by gridding all the observations to 2° x 2.5°. The combination of these observations is also aided by the fact that the retrieval algorithm for obtaining tropospheric NO<sub>2</sub> column density from all three instruments is the same

(<http://www.temis.nl/airpollution/no2.html>), and by the fact that their overpass times are similar (between 9:30 a.m. and 10:30 a.m. local time).

We tested our approach by inspecting the timeseries from individual  $2^\circ \times 2.5^\circ$  pixels over selected populated regions. These are shown in Figure D1.

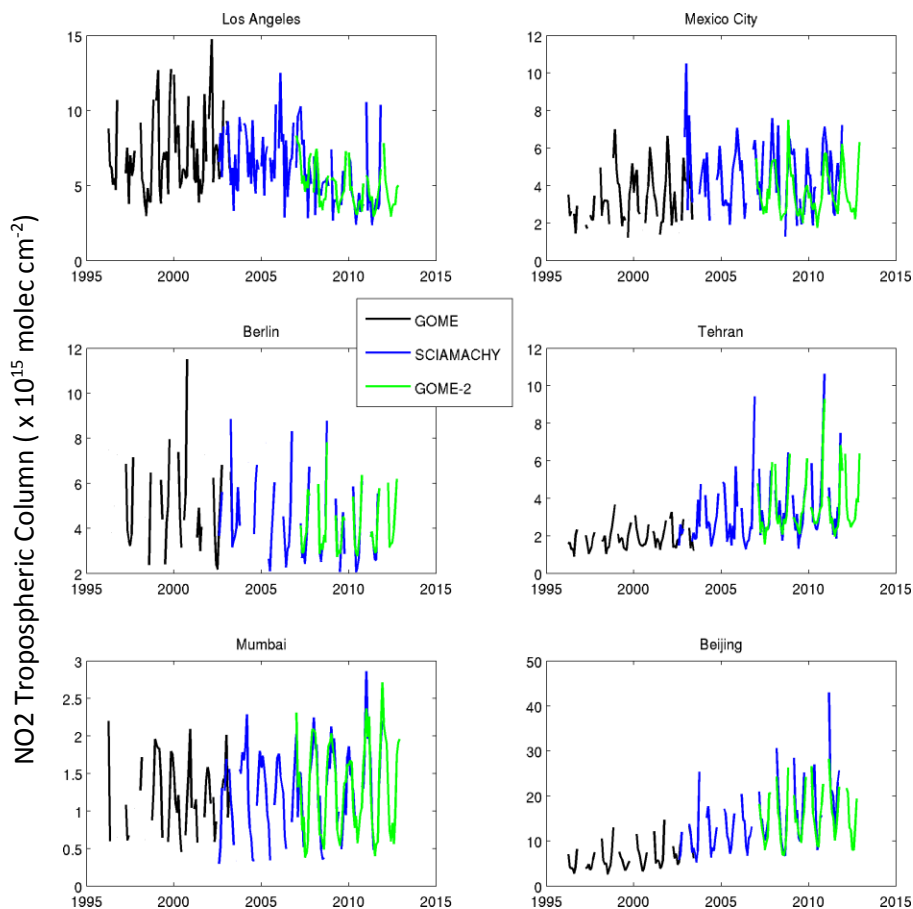


Figure D1: Monthly mean tropospheric NO<sub>2</sub> from GOME, SCIAMACHY, and GOME-2 show consistent agreement during overlap between instruments.

Given this and the consensus in the literature, we conclude that the instrumental differences between each satellite instrument are inconsequential to our analysis.

In response to the referee's comment, we have modified our manuscript to include additional citations, and to elaborate on our reasoning for combining the satellite instrument records despite their instrumental differences:

"We calculate top-down surface NO<sub>x</sub> emissions from 1996 to 2014 using observations from GOME (1995-2003), SCIAMACHY (2002-2011) and GOME-2 (2007- ). The similar overpass time of these three

instruments (from 9:30 a.m. to 10:30 a.m. local time) facilitates their combination to provide consistent long-term coverage (van der A et al., 2008; Konovalov et al. 2010; Geddes et al., 2016; Hilboll et al., 2013). We achieve consistency across all three instruments despite their varying pixel sizes (320 km x 40 km, 60 km x 30 km, and 80 km x 40 km for GOME, SCIAMACHY, and GOME-2 respectively) by gridding the daily observations from each to a regular coarse grid of 2° x 2.5° latitude by longitude.”

The referee also brings up the issue of changing a-priori vertical profiles over time. We agree that vertical profile shapes are an integral component of the tropospheric NO<sub>2</sub> column retrieval, and indeed are a significant contributor to column error (at least ~10% according to Boersma et al. (2004), and up to ~100% according to Laughner et al. (2016)). However, we are limited by the current generation of available global tropospheric NO<sub>2</sub> retrieval algorithms. Advances in satellite-derived tropospheric NO<sub>2</sub> column retrievals will be integral to improvements in top-down emissions estimates. In response to the reviewer comment, we address this in modifications we have made to the manuscript:

“The error in individual satellite-derived tropospheric NO<sub>2</sub> column retrievals to be around 35-60% for polluted scenes and greater than 100% for clean regions (Boersma et al. 2004).”

“We expect continued advancements in inversion approaches, satellite retrieval algorithms, and fundamental atmospheric chemistry processes will allow for increasingly accurate satellite-based constraints on deposition.”

**RC:** Page 4, Line 9: Since the topic of this Nowlan paper is similar and from the same group, it may be worth a sentence describing the major conclusion of this paper and how your manuscript is different/better. In fact, you may want to do briefly so the same for the other papers mentioned in this same paragraph.

**AC:** We thank the reviewer for this suggestion. We agree that it would be insightful to summarize the important points from Nowlan et al., although the statistical approaches taken by the other examples vary substantially from our approach and are less directly comparable. In response to this comment, we have included the following in our manuscript:

“Nowlan et al. (2014) demonstrated how satellite-inferred surface concentrations of NO<sub>2</sub> can be combined with modeling to produce spatially continuous estimates of NO<sub>2</sub> dry deposition fluxes. They found that dry deposition of NO<sub>2</sub> contributes as much as 85% of total NO<sub>y</sub> deposition in urban areas, but only represents 3% of global NO<sub>x</sub> emitted. The remaining 97% of global NO<sub>y</sub> deposition is made up of both wet and dry deposition of other reactive nitrogen oxide compounds that are not directly observed by satellite-based instruments.”

**RC:** Figure 2. The two rows of plots look identical. Is there any way to show the differences between the two periods. If not, I'm not sure it's helpful to show both rows.

**AC:** We are very grateful to the reviewer for their careful attention to this figure. In fact, the two panels are identical and this was an error in the original figure (both top and bottom accidentally show results for 2000-2002). We have corrected this mistake and sincerely apologise for the error. A new version of this figure will be uploaded with the corrected manuscript, and is included here as Figure D2 for the reviewer's reference. The differences between the two time periods are now more obvious. Declines in

wet nitrate deposition over this period are evident over North America and parts of Western Europe, while increases are evident over East Asia. Note that the observational coverage is also slightly different across the two periods.

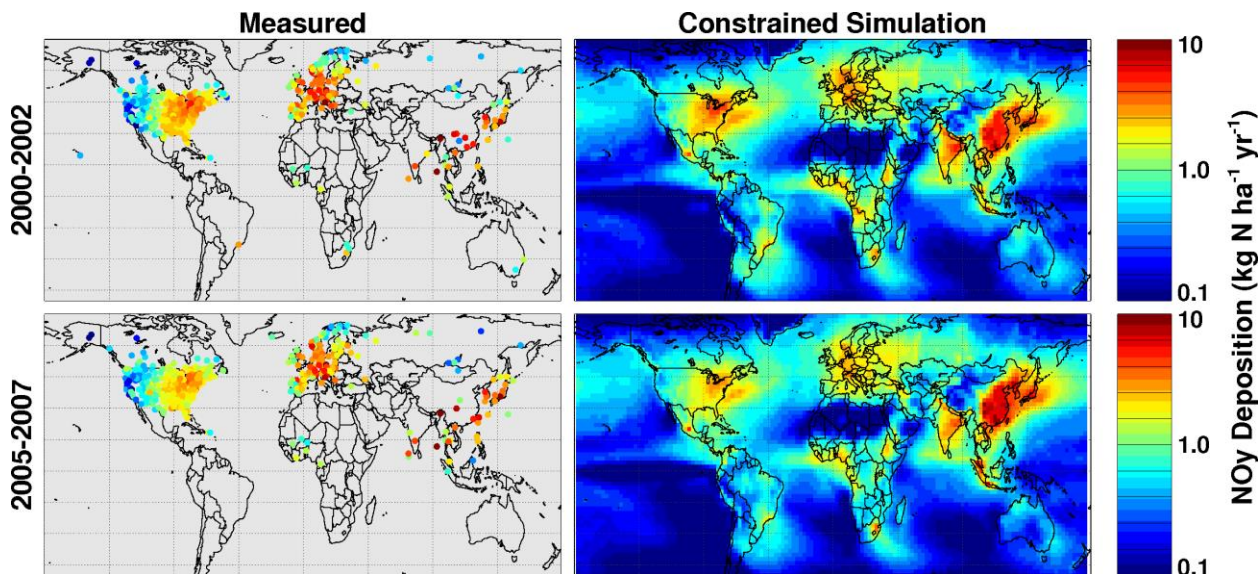


Figure D2: Corrected version of Figure 2 from the manuscript, showing results from the 2000-2002 comparison in the top panels, and results from the 2005-2007 comparison in the bottom panels.

#### REFERENCES:

- Benkovits et al. (1996), Global gridded inventories of anthropogenic emissions of sulfur and nitrogen, *Journal of Geophysical Research-Atmospheres*, 101, 29239–29253
- Irie et al. (2012), Quantitative bias estimates for tropospheric NO<sub>2</sub> columns retrieved from SCIAMACHY, OMI, and GOME-2 using a common standard for East Asia, *Atmospheric Measurement Techniques*, 5, 2403-2411
- Konovalov et al. (2010) Multi-annual changes of NO<sub>x</sub> emissions in megacity regions: nonlinear trend analysis of satellite measurement based estimates, *Atmos. Chem. Phys.*, 10, 8481–8498
- van der A et al. (2008), Trends, seasonal variability, and dominant NO<sub>x</sub> source derived from a ten year record of NO<sub>2</sub> measured from space, *Journal of Geophysical Research-Atmospheres*, 113, doi:10.1029/2007JD009021
- Zhao et al. (2017), Atmospheric nitrogen deposition to China: A model analysis on nitrogen budget and critical load exceedance, *Atmospheric Environment*, 153, 32-40
- Lin et al. (2010), Constraint of anthropogenic NO<sub>x</sub> emissions in China from different sectors: a new methodology using multiple satellite retrievals, *Atmos. Chem. Phys.*, 10, 63–78

Stavrakou et al. (2013), Key chemical NO<sub>x</sub> sink uncertainties and how they influence top-down emissions of nitrogen oxides, *Atmos Chem Phys*, 13, 9057-9082

Rienecker et al. (2011), MERRA: NASA's Modern-Era Retrospective Analysis for Research and Applications, *Journal of Climate*, 24, DOI: 10.1175/JCLI-D-11-00015.1

Reichle et al. (2017), Assessment of MERRA-2 land surface hydrology estimates, *Journal of Climate*, 30, DOI: 10.1175/JCLI-D-16-0720.1

Flechard et al. (2010), Dry deposition of reactive nitrogen to European ecosystems: a comparison of inferential models across the NitroEurope network, *Atmos Chem Phys*, 11, 2703-2728

Hardacre et al. (2015), An evaluation of ozone dry deposition in global scale chemistry climate models, *Atmos Chem Phys*, 15, 6419-6436

Schiferl et al. (2016), Interannual variability of ammonia concentrations over the United States: sources and implications, *Atmos Chem Phys*, 16, 12305-12328

# Global deposition of total reactive nitrogen oxides from 1996 to 2014 constrained with satellite observations of NO<sub>2</sub> columns

Jeffrey A. Geddes<sup>1,2</sup>, Randall V. Martin<sup>1,3</sup>

(1){Department of Physics and Atmospheric Science, Dalhousie University, Halifax, Nova Scotia, Canada}

(2){Now at: Department of Earth and Environment, Boston University, Boston, Massachusetts, USA}

(3){Harvard-Smithsonian Center for Astrophysics, Cambridge, Massachusetts, USA}

Correspondence to: J.A. Geddes (jgeddes@bu.edu)

## Abstract

Reactive nitrogen oxides (NO<sub>y</sub>) are a major constituent of the nitrogen deposited from the atmosphere, but observational constraints on their deposition are limited by poor or nonexistent measurement coverage in many parts of the world. Here we apply NO<sub>2</sub> observations from multiple satellite instruments (GOME, SCIAMACHY, and GOME-2) to constrain the global deposition of NO<sub>y</sub> over the last two decades. We accomplish this by producing top-down estimates of NO<sub>x</sub> emissions from inverse modeling of satellite NO<sub>2</sub> columns over 1996-2014, and including these emissions in the GEOS-Chem chemical transport model to simulate chemistry, transport, and deposition of NO<sub>y</sub>. Our estimates of long-term mean wet nitrate (NO<sub>3</sub><sup>-</sup>) deposition are highly consistent with available measurements in North America, Europe, and East Asia combined ( $r = 0.83$ , normalized mean bias = -7%,  $N = 136$ ). Likewise, our calculated trends in wet NO<sub>3</sub><sup>-</sup> deposition are largely consistent with the measurements, with 129 of the 136 gridded model-data pairs sharing overlapping 95% confidence intervals. We find that global mean NO<sub>y</sub> deposition over 1996-2014 is 56.0 Tg N yr<sup>-1</sup>, with a minimum in 2006 of 50.5 Tg N and a maximum in 2012 of 60.8 Tg N. Regional trends are large, with opposing signs in different parts of the world. Over 1996 to 2014, NO<sub>y</sub> deposition decreased by up to 60% in eastern North America, doubled in

1 regions of East Asia, and declined by 20% in parts of Western Europe. About 40% of the  
2 global  $\text{NO}_y$  deposition occurs over oceans, with deposition to the North Atlantic Ocean  
3 declining and deposition to the northwestern Pacific Ocean increasing. Using the residual  
4 between  $\text{NO}_x$  emissions and  $\text{NO}_y$  deposition over specific land regions, we investigate how  
5  $\text{NO}_x$  export via atmospheric transport has changed over the last two decades. Net export from  
6 the continental United States decreased substantially, from 2.9 Tg N  $\text{yr}^{-1}$  in 1996 to 1.5 Tg N  
7  $\text{yr}^{-1}$  in 2014. On the other hand, export from China more than tripled between 1996 and 2011  
8 (from 1.0 Tg N  $\text{yr}^{-1}$  to 3.5 Tg N  $\text{yr}^{-1}$ ), before a striking decline to 2.5 Tg N  $\text{yr}^{-1}$  by 2014. We  
9 find that declines in  $\text{NO}_x$  export from some Western European countries have counteracted  
10 increases in emissions from neighbouring countries to the east. A sensitivity study indicates  
11 that simulated  $\text{NO}_y$  deposition is robust to uncertainties in  $\text{NH}_3$  emissions with a few  
12 exceptions. Our novel long-term study provides timely context on the rapid redistribution of  
13 atmospheric nitrogen transport and subsequent deposition to ecosystems around the world.

14

## 15 **1 Introduction**

16 The introduction of reactive nitrogen to the environment by anthropogenic activities (e.g.  
17 from fossil fuel combustion and the production of fertilizers for agriculture) has drastically  
18 altered the global nitrogen cycle with consequences throughout the Earth system (Galloway  
19 2004). Reactive nitrogen dominates the chemical production of tropospheric ozone and  
20 contributes to inorganic aerosol formation, with implications for air quality and climate.  
21 Deposition of nitrogen from the atmosphere has been linked to eutrophication and  
22 acidification (Bouwman et al., 2002), reductions in biodiversity (Bobbink et al., 2010;  
23 Hernández et al., 2016; Isbell et al., 2013; De Schrijver et al., 2011), and climate impacts  
24 through coupling with the carbon cycle and greenhouse gas emissions (Liu and Greaver,  
25 2009; Reay et al., 2008; Templer et al., 2012). Despite its global importance, observational  
26 constraints on nitrogen deposition are lacking in many parts of the world due to poor or  
27 nonexistent measurement coverage (Vet et al., 2014).

28 Atmospheric transport is a dominant process for distributing reactive nitrogen around the  
29 world (Galloway et al., 2008). Some forms of reactive nitrogen can be transported over  
30 distances greater than 1000 km (Neuman et al., 2006; Sanderson et al., 2008), depositing  
31 across national boundaries and continents. For example, the U.S. is estimated to export 30-  
32 40% of its reactive nitrogen emissions (Dentener et al., 2006; Holland et al., 2005; Zhang et

1 al., 2012), while transport from China accounts for up to 66-92% of total nitrogen deposition  
2 to parts of the northwestern Pacific Ocean (Zhao et al., 2015). Fertilization of the open ocean  
3 due to atmospheric transport and deposition of anthropogenic nitrogen may be a considerable  
4 factor in marine productivity (Duce et al., 2008), prompting important questions about the fate  
5 and impact of deposition far downwind of sources where observations are limited.

6 Reactive nitrogen oxides ( $\text{NO}_y \equiv \text{NO} + \text{NO}_2 + \text{HNO}_3 + \text{HONO} + \text{organic nitrate}$   
7 molecules + aerosol nitrate) contribute about half of the total nitrogen deposited worldwide  
8 (Dentener et al., 2006).  $\text{NO}_y$  deposition was estimated to be around 45-50 Tg N yr<sup>-1</sup> in the  
9 late-1990s and early 2000s, representing a 3-4 fold increase since the pre-industrial era  
10 (Dentener et al., 2006; Kanakidou et al., 2016; Lamarque et al., 2013). A substantial range  
11 exists in the trajectory of global  $\text{NO}_y$  deposition beyond the year 2000 depending on emission  
12 scenario. Galloway et al. (2004) projected that  $\text{NO}_y$  deposition could increase by >70% by  
13 2050, while Dentener et al. (2006) projected changes between -25% to +50% by 2030 for  
14 maximum feasible reduction and “pessimistic” scenarios respectively. More recent multi-  
15 model projections by Lamarque et al. (2013) estimate  $\text{NO}_y$  deposition would change by -16%  
16 to +5% for 2030 and by -48% to -25% for 2100, depending on the Representative  
17 Concentration Pathway (RCP) scenario. This range in projections highlights the need for the  
18 global observational constraints on contemporary changes in nitrogen oxide emissions.

19 Sources of  $\text{NO}_x$  ( $\equiv \text{NO} + \text{NO}_2$ ), whose oxidation is responsible for the formation of other  
20 reactive nitrogen oxides, include fossil fuel combustion, biomass burning, lightning, and  
21 biogenic emission from soil. The magnitude and spatial distribution of  $\text{NO}_x$  emissions have  
22 changed considerably over the past several decades, corresponding to patterns of human  
23 development and emission control measures. Tropospheric  $\text{NO}_2$  columns derived from  
24 satellite remote sensing observations have been used extensively to constrain regional and  
25 global  $\text{NO}_x$  emissions (Streets et al., 2013). This top-down approach complements bottom-up  
26 inventories that are assembled using regionally specific emission factors and fuel combustion  
27 data for various source categories. In particular, satellite  $\text{NO}_2$  observations can provide insight  
28 into otherwise poorly constrained sources (Beirle et al., 2010; Jaegle et al., 2005; Richter et  
29 al., 2004; Vinken et al., 2014), produce coherent long-term trends (van der A et al., 2008; Lu  
30 et al., 2015; Stavrakou et al., 2008; Zhang et al., 2007), document interannual variability  
31 (Castellanos and Boersma, 2012; Konovalov et al., 2010a; Russell et al., 2012), offer  
32 information to evaluate and improve bottom-up inventories at the global scale (Martin, 2003;



1 Miyazaki et al., 2016), and provide timely emission updates (Lamsal et al., 2011; Mijling et  
2 al., 2013; Souri et al., 2016).

3 Satellite observations of NO<sub>2</sub> began with GOME (1995-2003) followed by  
4 SCIAMACHY (2002-2011), and continue today with OMI (2004- ), GOME-2 (2007- ), and  
5 TROPOMI (2017- ), resulting in a record of global atmospheric NO<sub>2</sub> abundance over the past  
6 20 years. These observations have been used previously to estimate the deposition of nitrogen  
7 species, either in combination with chemical transport modeling or with empirical approaches  
8 (Cheng et al., 2013; Jia et al., 2016; Lu et al., 2013; Nowlan et al., 2014). For example,  
9 Nowlan et al. (2014) demonstrated how satellite-inferred surface concentrations of NO<sub>2</sub> can  
10 be combined with modeling to produce spatially continuous estimates of NO<sub>2</sub> dry deposition  
11 fluxes. They found that dry deposition of NO<sub>2</sub> contributes as much as 85% of total NO<sub>y</sub>  
12 deposition in urban areas, but represents only 3% of global NO<sub>x</sub> emitted. The remaining 97%  
13 of global NO<sub>y</sub> deposition is made up of both wet and dry deposition of other reactive nitrogen  
14 oxide compounds that are not directly observed by satellite-based instruments.

15 In this study, we expand on the approach of Nowlan et al. (2014) by using the satellite  
16 observations of NO<sub>2</sub> columns to constrain total NO<sub>y</sub> deposition, including other oxidized  
17 nitrogen species and wet deposition which contribute substantially to NO<sub>y</sub> deposition. We  
18 accomplish this by constraining surface NO<sub>x</sub> emissions using the satellite observations of  
19 NO<sub>2</sub>, and simulating subsequent NO<sub>y</sub> deposition with a global chemical transport model.  
20 Given the effective mass balance between NO<sub>x</sub> emissions and deposition of reactive nitrogen  
21 oxides, observational constraints on NO<sub>x</sub> emissions provide a powerful top-down constraint  
22 on deposition (which to our knowledge has not yet been exploited in this way).

23 We leverage the long-term coverage of GOME, SCIAMACHY, and GOME-2  
24 observations to produce a globally consistent and continuous record of NO<sub>y</sub> deposition from  
25 1996 to 2014. We highlight long-term trends in satellite-constrained NO<sub>y</sub> deposition around  
26 the world and discuss changes in regional export of NO<sub>x</sub>. Our satellite-constrained estimates  
27 of NO<sub>y</sub> deposition are evaluated using measured wet nitrate (NO<sub>3</sub><sup>-</sup>) deposition from a variety  
28 of sources worldwide. We also explore the sensitivity of the NO<sub>y</sub> deposition estimates to  
29 uncertainties in NH<sub>3</sub> emissions.

30

## 1 2 Methods

### 2 2.1 Satellite-based constraints on NO<sub>y</sub> deposition

3 The application of satellite NO<sub>2</sub> column observations to constrain NO<sub>y</sub> deposition  
4 requires a method to propagate the observational information across the entire NO<sub>y</sub> system  
5 containing species with lifetimes of days or longer. The short NO<sub>x</sub> lifetime of hours during  
6 daytime satellite observations implies that a direct assimilation for NO<sub>2</sub> column abundance  
7 would rapidly lose the observational information as the assimilation returns to its unperturbed  
8 state well before the next satellite observation days later. We therefore apply satellite NO<sub>2</sub>  
9 observations to constrain NO<sub>x</sub> emissions in a simulation of NO<sub>y</sub> deposition so the information  
10 propagates across the entire NO<sub>y</sub> system.

11 We calculate top-down surface NO<sub>x</sub> emissions from 1996 to 2014 using observations  
12 from GOME (1995-2003), SCIAMACHY (2002-2011) and GOME-2 (2007- ). The similar  
13 overpass time of these three instruments (from about 9:30 a.m. to 10:30 a.m. local time)  
14 facilitates their combination to provide consistent long-term coverage (Geddes et al., 2015;  
15 Hilboll et al., 2013; Konovalov et al. 2010; van der A et al., 2008). We achieve consistency  
16 across all three instruments despite their varying pixel sizes (320 km x 40 km, 60 km x 30 km,  
17 and 80 km x 40 km for GOME, SCIAMACHY, and GOME-2 respectively) by gridding the  
18 daily observations from each to a regular coarse grid of 2° x 2.5° latitude by longitude.  
19 Tropospheric NO<sub>2</sub> vertical column densities are provided by KNMI at  
20 <http://www.temis.nl/airpollution/>. In all cases, NO<sub>2</sub> column densities are retrieved by  
21 differential optical absorption spectroscopy using backscattered radiance in the 425-450 nm  
22 wavelength range according to the retrieval algorithm documented in Boersma et al. (2004).  
23 The error in individual satellite-derived tropospheric NO<sub>2</sub> column retrievals to be around 35-  
24 60% for polluted scenes and greater than 100% for clean regions (Boersma et al. 2004).  
25 Boersma et al. (2016) well describe the value of accounting for vertically-resolved instrument  
26 sensitivity. We use the averaging kernels provided with the data to replace a priori NO<sub>2</sub>  
27 vertical profiles with those from GEOS-Chem model following Lamsal et al. (2010). We use  
28 daily nadir observations with a cloud radiance fraction of less than 0.5. We minimize errors  
29 associated with wintertime retrievals by using a solar zenith angle cut-off of 50°.

30 We use the GEOS-Chem chemical transport model ([www.geos-chem.org](http://www.geos-chem.org)) v9-02 to  
31 conduct the inversion of satellite observations of NO<sub>2</sub> and constrain global NO<sub>y</sub> deposition.

1 The simulation is described in Appendix 1. Briefly, GEOS-Chem is driven by assimilated  
2 meteorology from the NASA Global Modeling and Assimilation Office and simulates  
3 detailed HO<sub>x</sub>-NO<sub>x</sub>-VOC-aerosol chemistry (Bey et al., 2001; Park et al., 2004). Removal  
4 occurs through wet deposition (Amos et al., 2012; Liu et al., 2001), and dry deposition based  
5 on the widely used resistance-in-series formulation (Wesely, 1989). Anthropogenic, biogenic,  
6 soil, lightning, and biomass burning emissions are included (see Appendix 1). In the case of  
7 NO<sub>x</sub>, the bottom-up emissions are used as prior estimates that we then overwrite with the top-  
8 down emissions.

9 We adopt a finite-difference mass balance inversion (Cooper et al., 2017; Lamsal et al.,  
10 2011) for computational expedience given the 19-year period of interest. In two initial  
11 simulations, a perturbation (30%) to the a-priori emissions,  $E$ , in a grid cell is used to find the  
12 relationship between the a-priori NO<sub>2</sub> column,  $\Omega$ , and the change in the column resulting from  
13 that perturbation:

$$14 \quad \frac{\Delta E}{E} = \beta \times \frac{\Delta \Omega}{\Omega} \quad (1)$$

15 The factor  $\beta$  in Equation 1 accounts for non-linear feedbacks between a change in NO<sub>x</sub>  
16 emissions and NO<sub>x</sub> chemistry in a grid cell leading to grid cell NO<sub>2</sub> column abundance.

17 We then use monthly-mean gridded satellite observations,  $\Omega_{sat}$ , in combination with  
18 monthly  $\beta$  values for each grid box to derive new gridded annual emissions,  $E_{topdown}$ , from the  
19 prior emissions estimates,  $E_{prior}$ , by rewriting Equation 1 as:

$$20 \quad E_{topdown} = E_{prior} \cdot \left[ 1 - \beta \frac{\Omega_{sat} - \Omega_{prior}}{\Omega_{prior}} \right] \quad (2)$$

21 We use GOME observations for years 1996 to 2002, SCIAMACHY observations for years  
22 2003 to 2006, and GOME-2 observations for years 2007 to 2014. In all cases, monthly mean  
23 simulated NO<sub>2</sub> columns are calculated using days with coincident satellite observations. The  
24 simulated NO<sub>2</sub> vertical column is output daily for late morning. We calculate ~~annual-mean~~  
25 scaling factors for every month with available satellite observations, then calculate an annual  
26 mean scaling factor that is used to infer annual mean ~~from the mean monthly~~ top-down  
27 emissions. Our top-down emissions retain the same seasonality as the prior emissions to  
28 mitigate concerns about seasonally missing data (such as from snow or monsoonal clouds).  
29 The top-down emissions are then used in a final simulation to model NO<sub>y</sub> deposition. For

1 locations without any satellite observations, the a-priori emissions are used. The resultant  
2 simulation of NO<sub>y</sub> deposition is thus constrained by, and consistent with, the satellite NO<sub>2</sub>  
3 observations (similar in essence to an assimilation system). We note uncertainty in  
4 tropospheric NO<sub>2</sub> from lightning will propagate into the inversion (Travis et al., 2016)(~~Travis  
5 et al. 2016~~), but there is no evidence of a significant trend in lightning NO<sub>x</sub> over the long term  
6 (Murray et al. 2012). A constant bias is unlikely to affect the trend analyses presented here.

7 Table 1 shows the annual global top-down NO<sub>x</sub> emissions we obtain from our  
8 calculations. We derive global mean satellite-constrained NO<sub>x</sub> emissions from 1996-2014 of  
9 553.62 ± 3.4 Tg N yr<sup>-1</sup>. Our top-down global NO<sub>x</sub> emissions for 2001 of 520.30 Tg N are  
10 consistent with the mean ± standard deviation from over 20 models used in the Coordinated  
11 Model Studies Activities of the Task Force on Hemispheric Transport of Air Pollution  
12 (HTAP) for the same year of 46.6 ± 7.8 Tg N (Vet et al. 2014).

## 13 **2.2 Measurements of Wet Deposition**

14 We use a variety of regional and global measurements of wet nitrate (NO<sub>3</sub><sup>-</sup>) deposition  
15 to evaluate our satellite-constrained simulation from 1996 to 2014.

16 To evaluate overall global performance we use data compiled by the World Data Centre  
17 for Precipitation Chemistry for two time periods: 2000-2002 and 2005-2007  
18 (<http://www.wdpc.org/>). The use of this data ensures optimal and consistent quality  
19 standards across all stations, allowing for evaluation of global performance with careful  
20 consideration of sampling protocols and data completeness (Vet et al. 2014).

21 To evaluate the long-term means and trends from 1996-2014, we obtain observations of  
22 wet NO<sub>3</sub><sup>-</sup> deposition from North America, Europe, and East Asia where continuous  
23 measurements are available throughout most of our study period. Observations come from the  
24 National Atmospheric Deposition Program in the United States (<http://nadp.sws.uiuc.edu/>,  
25 available 1996-2014), from the Canadian Air and Precipitation Monitoring Network in  
26 Canada (<http://www.ec.gc.ca/rs-mn/>, available 1996-2011), from the European Monitoring  
27 and Evaluation Programme in Europe (<http://www.emep.int/>, available 1996-2014) and from  
28 the Acid Deposition Monitoring Network in East Asia (<http://www.eanet.asia>, available 2000-  
29 2014). In the US and Canada, wet deposition is measured by wet-only samplers that are  
30 triggered at the onset of precipitation. Measurements in Europe are made by bulk- and wet-  
31 only sampling methods and we used both in this analysis. Measurements across East Asia are

1 reported as wet-only, although at some stations this may not be accomplished by strictly wet-  
2 only samplers (<http://www.eanet.asia/product/manual/prev/techwet.pdf>).

3 For our analysis, we only included stations which had quality controlled annual data for  
4 at least 15 of the 19 years in our study. This left 128 stations across the United States, 14  
5 stations in Canada, 18 stations across Europe, and 14 stations across East Asia. For  
6 comparison with the GEOS-Chem model, if multiple stations are available within a single  
7 grid box we grid all measurements of annual wet deposition to the model horizontal  
8 resolution.

9

### 10 **3 Satellite-Constrained Estimates of NO<sub>y</sub> Deposition**

11 Here we summarize the overall patterns in long-term mean deposition resulting from our  
12 satellite-constrained simulation, followed by a discussion of the long term trends, changes in  
13 regional export, and the sensitivity of the simulated NO<sub>y</sub> deposition to potential uncertainties  
14 in NH<sub>3</sub> emissions.

#### 15 **3.1 Long-term Mean NO<sub>y</sub> Deposition**

16 Figure 1 (top) shows our satellite-constrained long-term mean NO<sub>y</sub> deposition from  
17 1996 to 2014. We find that 32.2 Tg N yr<sup>-1</sup> is deposited on average over the continents (57% of  
18 the total), and 23.8 Tg N yr<sup>-1</sup> is deposited on average over the oceans (43% of the total). This  
19 is similar to the estimate by Galloway et al. (2004) that 46% of modern day NO<sub>y</sub> deposition  
20 occurs over the oceans. Critical nitrogen deposition loads for various natural freshwater and  
21 terrestrial ecosystems lie in the range of 5-20 kg N ha<sup>-1</sup> yr<sup>-1</sup>, depending on the ecosystem, soil  
22 conditions, and land history (World Health Organization, 2000). We estimate that mean  
23 deposition of oxidized nitrogen alone exceeds 5 kg N ha<sup>-1</sup> yr<sup>-1</sup> over a land area of  
24 approximately 12.7 x 10<sup>6</sup> km<sup>2</sup> (or ~8% total land area).

25 In the Northern Hemisphere, high NO<sub>y</sub> deposition tends to be associated with regions  
26 that have high anthropogenic NO<sub>x</sub> sources. We find mean NO<sub>y</sub> deposition in the eastern  
27 United States exceeds 10 kg N ha<sup>-1</sup> yr<sup>-1</sup> (maximum = 11.4 kg N ha<sup>-1</sup> yr<sup>-1</sup>) with elevated  
28 deposition extending into southeastern Canada and hundreds of kilometers into the Atlantic  
29 Ocean. This is similar to the multi-model ensemble results from ACCMIP and HTAP,  
30 predicting between 5-15 kg N ha<sup>-1</sup> yr<sup>-1</sup> in this region (Lamarque et al. 2013; Vet et al. 2014).

1 A prior GEOS-Chem analysis over North America for the years 2006-2008 also predicted  
2  $\text{NO}_y$  deposition exceeding  $10 \text{ kg N ha}^{-1} \text{ yr}^{-1}$  in the eastern US (Zhang et al. 2012). Elsewhere  
3 in North America, we find high  $\text{NO}_y$  deposition along the west coast of California (up to  $6 \text{ kg}$   
4  $\text{N ha}^{-1} \text{ yr}^{-1}$ ) and in the vicinity of Mexico City (up to  $10 \text{ kg N ha}^{-1} \text{ yr}^{-1}$ ).

5 We find mean  $\text{NO}_y$  deposition is also elevated throughout Europe, with a maximum of  
6  $8.5 \text{ kg N ha}^{-1} \text{ yr}^{-1}$  located in northern Italy near the Po Valley region. Again, our long-term  
7 estimate in this region is similar to the ACCMIP and HTAP ensemble means, predicting  $\text{NO}_y$   
8 deposition in the range of  $5\text{-}10 \text{ kg N ha}^{-1} \text{ yr}^{-1}$  (Lamarque et al. 2013; Vet et al. 2014). The  
9 elevated deposition here is also spatially consistent with the results from Holland et al. (2005).  
10 We find high deposition extending into western Russia with a hotspot in the vicinity of  
11 Moscow approaching  $5 \text{ kg N ha}^{-1} \text{ yr}^{-1}$ . Our observation-constrained estimate also has isolated  
12 regions of high deposition in the Middle East (around  $4\text{-}5 \text{ kg N ha}^{-1} \text{ yr}^{-1}$  in the vicinity of  
13 Tehran and around the Persian Gulf).

14 We find that the highest mean deposition in the world occurs in China, exceeding  $10 \text{ kg}$   
15  $\text{N ha}^{-1} \text{ yr}^{-1}$  in many regions. High deposition extends into the mid-latitude western Pacific  
16 Ocean off the coast of East Asia.  $\text{NO}_y$  deposition in the ACCMIP and HTAP ensemble means  
17 also exceeds  $10 \text{ kg N ha}^{-1} \text{ yr}^{-1}$  throughout eastern China. We find the highest long-term mean  
18 deposition (with a maximum close to  $20 \text{ kg N ha}^{-1} \text{ yr}^{-1}$ ) occurs in the south, around the Pearl  
19 River Delta and in the vicinity of Guangzhou, although deposition is also high in the regions  
20 just west of Beijing and Shanghai.

21 In the Southern Hemisphere, high  $\text{NO}_y$  deposition is associated with biomass burning  
22 and soil  $\text{NO}_x$  sources, in addition to anthropogenic sources. For example, we find  $\text{NO}_y$   
23 deposition is between  $3$  to  $5 \text{ kg N ha}^{-1} \text{ yr}^{-1}$  in central and southern Brazil, and in the tropical  
24 rainforests and moist savannahs of Africa. Our estimates in these biomass burning and soil  
25  $\text{NO}_x$  dominated regions are also generally consistent with the ACCMIP and HTAP ensemble  
26 estimates ( $2\text{-}5 \text{ kg N ha}^{-1} \text{ yr}^{-1}$ ). We find  $\text{NO}_y$  deposition up to  $10 \text{ kg N ha}^{-1} \text{ yr}^{-1}$  in the vicinity of  
27 Sao Paulo and Rio de Janeiro, and in the vicinity of Johannesburg and the industrialized  
28 Mpumalanga Highveld of South Africa (all dominated by anthropogenic  $\text{NO}_x$  emissions). Our  
29 constrained simulation also identifies hotspots of deposition in the vicinity of Melbourne and  
30 Sydney, Australia ( $\sim 4 \text{ kg N ha}^{-1} \text{ yr}^{-1}$ ).

31 Figure 1 (bottom) shows the simulated long-term ratio of dry  $\text{NO}_y$  deposition to total  
32 (wet + dry)  $\text{NO}_y$  deposition. Globally, dry and wet deposition contribute roughly equally to

1 total  $\text{NO}_y$  deposition (52% and 48% respectively). Dry deposition usually accounts for more  
2 than 50% of the total over the continents and directly off shore whereas wet deposition  
3 dominates over the remote oceans. In the generally arid regions of the world (e.g.  
4 southwestern US, the Sahara Desert, the Arabian Peninsula, and the Gobi Desert) dry  
5 deposition accounts for ~85% or more of the total deposition. Elsewhere, dry deposition  
6 fractions tend to be highest (>60%) nearest to major surface  $\text{NO}_x$  sources (e.g. eastern US,  
7 Western Europe, and near other major urban centres around the world in addition to the soil  
8 and biomass-burning dominated source regions in South America and Africa).  $\text{HNO}_3$   
9 typically makes the dominant contribution to dry  $\text{NO}_y$  deposition, although  $\text{NO}_2$  and  $\text{HNO}_3$   
10 can make almost equal contributions in certain high- $\text{NO}_x$  environments. Isoprene nitrates and  
11 peroxyacetyl nitrates comprise ~10-30% of dry  $\text{NO}_y$  deposition in some densely forested and  
12 high latitude environments respectively.

13 We evaluate our estimates of  $\text{NO}_y$  deposition with measured wet  $\text{NO}_3^-$  from several  
14 sources. Figure 2 shows measurements of annual wet  $\text{NO}_3^-$  deposition from the World Data  
15 Centre for Precipitation Chemistry, available for two time periods: 2000-2002 (N = 470) and  
16 2005-2007 (N = 484). In both we see the patterns of elevated deposition in eastern North  
17 America, Western Europe, and parts of South and East Asia, with lower deposition in western  
18 North America, across high latitudes in the Northern Hemisphere, and in the available  
19 observations in Africa. High deposition in the Southern Hemisphere is observed between Sao  
20 Paulo and Rio de Janeiro, and just southeast of Johannesburg. Figure 2 also shows the wet  
21  $\text{NO}_3^-$  deposition from our constrained simulation during the same two time periods (2000-  
22 2002 and 2005-2007), which exhibits similar patterns found in total  $\text{NO}_y$  deposition (Figure  
23 1).

24 We find a high degree of consistency between our estimate and the observations for  
25 both the 2000-2002 (N = 306 model-data pairs) and 2005-2007 (N = 310 model-data pairs).  
26 ~~The Normalized-normalized~~ mean bias (NMB) is -14% and -16% respectively. The vast  
27 majority of pairs (> 80%) agree to within 50% of each other. Figure 3 shows scatter plots for  
28 specific subsets of the global data. The agreement for both time periods is strongest over  
29 North America ( $r = 0.92$  for both 2000-2002 and 2005-2007, NMB = +1.0% and -5.0%  
30 respectively). Robust model agreement with wet nitrate deposition observations over densely  
31 monitored North America is characteristic of other global studies (Dentener et al. 2006;  
32 Lamarque et al. 2013; Vet et al. 2014). Our agreement is also good in Europe ( $r = 0.69$  and

1 0.66, and NMB = -31.0% and -29.8% respectively). The weaker correlation and low bias in  
2 this region is likewise characteristic of global studies, although our spatial correlation ( $r=0.66$ -  
3  $0.69$ ) is on the high end of previously reported multi-model ensembles ( $r \sim 0.4$ - $0.6$ , Dentener  
4 et al. 2006; Lamarque et al. 2013; Vet et al. 2014). The negative bias over Europe compared  
5 to North America has previously been attributed to poor modeling of precipitation, and/or  
6 spatial representativeness of the measurements compared to model resolution. Throughout the  
7 rest of the world (encompassing observations mostly over Asia, but also over eastern Russia,  
8 and some locations in the Southern Hemisphere) the combined spatial coverage of the  
9 observations is very low ( $N = 53$ ). Normalized mean bias in these estimates is also high  
10 compared to North America (NMB = -19.5% and -17.8% for 2000-2002 and 2005-2007  
11 respectively), and our spatial correlation with the measurements is weak ( $r = 0.35$  and  $0.42$   
12 respectively). We find that our poor agreement here is disproportionately driven by the two  
13 observations that also have the highest measured deposition in the world: near Port Blair on  
14 the South Andaman Island in the Bay of Bengal, and in the Arunachal Pradesh state in  
15 northeastern India. Agreement is considerably better with the rest of the data ( $r = 0.78$  and  
16  $0.72$ , NMB = +0.01% and -0.01% for 2000-2002 and 2005-2007 respectively). Excluding  
17 these two points substantially improves the global agreement as well (from  $r = 0.57$  to  $0.75$   
18 and  $r = 0.59$  to  $0.75$  respectively). Site representativeness, precipitation errors, or uncertainty  
19 in our satellite-constrained  $\text{NO}_x$  emissions may explain the discrepancy at these two specific  
20 sites.

21 In addition to global data for 2000-2002 and 2005-2007 from the World Data Centre for  
22 Precipitation Chemistry, we also evaluate our estimates of  $\text{NO}_y$  deposition over the long-term  
23 (1996-2014) using continuous observations provided by regional networks. Figure 4 shows  
24 measured wet  $\text{NO}_3^-$  deposition over North America, Europe, and East Asia for locations where  
25 at least 15 years of quality-controlled annual data are available. These long-term mean  
26 observations demonstrate many of the same spatial patterns as the time slices from 2000-2002  
27 and 2005-2007. In North America, a relatively smooth gradient is observed from low  
28 deposition in the west to high deposition at sites in the east. In Europe, the highest measured  
29 long-term mean wet  $\text{NO}_3^-$  deposition occurs at a coastal site in southern Norway, at a site just  
30 east of Copenhagen, and at locations in northern Italy and in Switzerland. At higher latitude  
31 sites, deposition is lower. Across the eastern Asia network, the measurements show highest  
32 deposition at sites in Southeast Asia (e.g. at a location between Kuala Lumpur and Singapore,  
33 and another in the vicinity of Jakarta) and in Japan. The lowest long-term mean deposition



1 occurs at high latitude sites along the border of Russia and Mongolia, while moderate to high  
2 deposition is measured on the coast of eastern China.

3 In general, our satellite-constrained estimate reflects the spatial variability that is seen in  
4 the measurements. Globally, the correlation between measured  $\text{NO}_3^-$  deposition and our  
5 estimated wet  $\text{NO}_3^-$  deposition is excellent ( $r = 0.83$ ,  $\text{NMB} = -7.7\%$ ,  $N = 136$  gridded model-  
6 data pairs). The vast majority of pairs ( $> 85\%$ ) agree to within 50% of each other. For the  
7 individual regions, normalized mean bias in our estimate is smallest over North America  
8 ( $\text{NMB} = +2.4\%$ ), and higher over Europe and East Asia ( $\text{NMB} = -32\%$  and  $-25\%$   
9 respectively). The spatial correlation over each region is strong ( $r = 0.89$ ,  $r = 0.87$ , and  $r =$   
10  $0.69$  for North America, Europe, and East Asia respectively), but sample sizes over Europe ( $N$   
11  $= 16$ ) and East Asia ( $N = 11$ ) are small so we emphasize caution in the interpretation of the  
12 statistics for these two regions. The lack of continuous measurement coverage even in parts of  
13 the world with routine network observations highlights the imperative of using other novel  
14 observational constraints on deposition (such as the global satellite observations of  $\text{NO}_2$  used  
15 here).

### 16 **3.2 Trends in Global $\text{NO}_y$ Deposition from 1996 to 2014**

17 Our long-term satellite-constrained estimate of  $\text{NO}_y$  deposition facilitates a unique and  
18 up-to-date investigation of the changes in  $\text{NO}_y$  deposition around the world. We calculate  
19 linear trends in annual  $\text{NO}_y$  deposition using the nonparametric Sen's method (Sen, 1968),  
20 and test for significance with the nonparametric Mann-Kendall method (Kendall, 1975;  
21 Mann, 1945). We treat increasing or decreasing trends as significant if  $p < 0.01$ . Given that  
22 this is a test for linear trends, regions where shorter-term trends in deposition may have  
23 changed signs over the period of study could result in erroneous or insignificant trends. Below  
24 we discuss particular regions where this is the case.

25 Figure 5 shows the long-term annual and seasonal trends calculated from our satellite-  
26 constrained estimate of total  $\text{NO}_y$  deposition across 1996-2014 (hatching indicates statistical  
27 significance). Figure 6 highlights timeseries of total  $\text{NO}_y$  deposition over three specific  
28 regions covering parts of North America, Western Europe, and East Asia (as outlined in  
29 dashed boxes in the top panel of Fig. 5).

30 Substantial decreases are seen throughout North America extending over the Atlantic  
31 Ocean to remote regions. The timeseries for this region (Fig. 6, left) shows that  $\text{NO}_y$

1 deposition decreased by almost 40% from 6.4 Tg N yr<sup>-1</sup> in 1996-1998 to 3.9 Tg N yr<sup>-1</sup> in  
2 2012-2014. The steepest local decline in the world appears over the Ohio River Valley area,  
3 with a maximum near Pittsburgh where NO<sub>y</sub> deposition decreased by -0.6 kg N ha<sup>-1</sup> yr<sup>-2</sup>. NO<sub>y</sub>  
4 deposition near Pittsburgh decreased from consistently exceeding 15 kg N ha<sup>-1</sup> yr<sup>-1</sup> during  
5 1996-2000, to below 6 kg N ha<sup>-1</sup> yr<sup>-1</sup> by 2014. The strong decrease in the northeast is  
6 consistent with other long-term observational studies for the US (Sickles II and Shadwick,  
7 2007, 2015). Studies of US NO<sub>x</sub> emissions derived from satellite observations have also  
8 highlighted the remarkable success of emission controls (Duncan et al., 2013; Russell et al.,  
9 2012). Our constrained estimate has the steepest declines during the summer (Fig 5, JJA),  
10 restricted tightly to the source regions. This also agrees with long-term observations showing  
11 the strongest reductions in the summer (Sickles II and Shadwick 2015), consistent with the  
12 shorter lifetime of NO<sub>x</sub> and efficient dry deposition of NO<sub>y</sub> over the forested eastern US. We  
13 find significant decreases far downwind over the Atlantic Ocean during the other months,  
14 when NO<sub>y</sub> can be transported farther. The steep change in NO<sub>y</sub> deposition in the eastern US  
15 over the last 20 years may have important consequences on tree mortality rates in the region,  
16 which have been demonstrated to be very sensitive to NO<sub>3</sub><sup>-</sup> deposition in the range of 5-15 kg  
17 N ha<sup>-1</sup> yr<sup>-1</sup> (Dietze and Moorcroft, 2011). The steeply decreasing trends across the US in our  
18 satellite-derived NO<sub>y</sub> also support the increasing dominance of reduced nitrogen in total  
19 nitrogen deposition evidenced by observations (Li et al., 2016) and model predictions (Ellis et  
20 al., 2013).

21 We find a small but statistically significant positive trend in NO<sub>y</sub> deposition (+0.06 kg  
22 N ha<sup>-1</sup> yr<sup>-2</sup>) in northern Alberta, Canada, dominated by the trend in JJA. The region is  
23 downwind of development in the Canadian oil sands, which has seen notable changes in NO<sub>2</sub>  
24 column abundance as observed from space (McLinden et al., 2012). We estimate that  
25 deposition of NO<sub>y</sub> in this area was at a maximum of 3.4 kg N ha<sup>-1</sup> yr<sup>-1</sup> in 2011 (up from 1.3 kg  
26 N ha<sup>-1</sup> yr<sup>-1</sup> in 1996-1997), and has since declined to 1.6 kg N ha<sup>-1</sup> yr<sup>-1</sup> by 2014. Elsewhere in  
27 Canada we estimate that NO<sub>y</sub> deposition has decreased in the south and east parts of the  
28 country, consistent with observational analyses (Zbieranowski and Aherne, 2011).

29 Declines in NO<sub>y</sub> deposition are also found across Europe, but statistical significance  
30 tends to be limited to western continental Europe and the United Kingdom (while changes in  
31 the south, north, and eastern countries tend to be insignificant). According to the timeseries  
32 for this region (Fig. 6, middle), NO<sub>y</sub> deposition decreased by about 15% (from 2.5 Tg N yr<sup>-1</sup>

1 in 1996-1998 to 2.1 Tg N yr<sup>-1</sup> in 2012-2014). We find the steepest local trends (-0.1 kg N ha<sup>-2</sup>  
2 yr<sup>-1</sup>) in eastern Germany and southern UK, where NO<sub>y</sub> deposition in 2012-2014 decreased by  
3 20% compared to 1996-1998. Previous satellite constraints on NO<sub>x</sub> emissions established that  
4 NO<sub>x</sub> emissions in France, Germany, Great Britain, and Poland have declined since 1996 while  
5 emissions in Greece, Italy, Spain, and the Ukraine for example have either stayed constant or  
6 increased (Konovalov et al., 2008). The local variability in emission trends leads to notable  
7 transboundary impacts. For example, our simulation predicts no net trend in NO<sub>y</sub> deposition  
8 over the Ukraine; but we find this is a result of opposing trends in dry (increasing) and wet  
9 (decreasing) deposition. This would be explained by increasing local emissions but decreasing  
10 transport from upwind. Similarly, we find significant increases in dry deposition in parts of  
11 western Russia but no significant trend in wet deposition.

12 Large increases in NO<sub>y</sub> deposition are found throughout Asia, concentrated especially in  
13 eastern China and parts of Southeast Asia. Figure 6 shows the timeseries of wet and dry NO<sub>y</sub>  
14 deposition within the rectangular region outlined in Figure 5 that encompasses eastern China  
15 and part of the adjacent ocean. We find that NO<sub>y</sub> deposition in the region increased by 65%  
16 from 5.2 Tg N yr<sup>-1</sup> in 1996-1998 to 8.6 Tg N yr<sup>-1</sup> in 2012-2014. The timeseries also shows  
17 that NO<sub>y</sub> deposition decreased after peaking around 9.3 Tg N yr<sup>-1</sup> in 2011-2012. We find that  
18 the steepest increasing local trends in the world appear in eastern China, and in the Pearl  
19 River Delta region (up to +0.6 kg N ha<sup>-1</sup> yr<sup>-2</sup>). In fact, deposition in the Pearl River Delta  
20 region is the highest in the world for most of our record, exceeding 20 kg N ha<sup>-1</sup> yr<sup>-1</sup> every  
21 year from 2003-2014 (almost doubling from just over 11 kg N ha<sup>-1</sup> yr<sup>-1</sup> in 1996). The trends in  
22 deposition over China are largest in summer when the NO<sub>x</sub> lifetime is short, with more  
23 obvious indications of increasing NO<sub>y</sub> transport/export in the spring months (Fig 5, MAM).  
24 The substantial increase in NO<sub>x</sub> emissions throughout East Asia has been inferred from  
25 satellite instruments in several previous studies (Mijling et al., 2013; Richter et al., 2005).  
26 The timing and extent of the reversal in NO<sub>y</sub> deposition that we see is also consistent with  
27 observed NO<sub>2</sub> columns over eastern China derived from OMI (de Foy et al., 2016; Krotkov et  
28 al., 2016). The ability of our satellite-constrained NO<sub>y</sub> deposition estimate to capture this  
29 sudden dramatic decrease over China, in contrast with previous projections (e.g. the RCP2.6,  
30 RCP4.5, and RCP8.5 projections to 2030, Lamaque et al. 2013), emphasizes an attribute of  
31 the satellite constraint.

1 Small statistically significant decreasing trends are found over the biomass-burning  
2 dominated source regions of Africa. The decrease in  $\text{NO}_y$  deposition of about  $\sim 3\% \text{ yr}^{-1}$   
3 relative to the long-term mean in Northern Africa is consistent with the most recent GFED4  
4 inventory from 1997 to 2014 (<http://www.globalfiredata.org/>), which has fire  $\text{NO}_x$  emissions  
5 decreasing at a rate of about  $3\% \text{ yr}^{-1}$  in this region. In contrast, we also estimate a similar  
6 decrease in Southern Africa that is not represented in the recent GFED4 emission timeseries.  
7 A reduction in  $\text{NO}_2$  column abundance in this region (observed by GOME and  
8 SCIAMACHY) was also reported by van der A. (2008). They postulate that this decline could  
9 be a result of deforestation leading to less biomass burning, but changing  $\text{NO}_x$  emission  
10 factors from biomass burning could also potentially ~~explain~~ contribute to the trend.

11 Despite the large regional trends described above, we find that global deposition  
12 changed very little between 1996-1998 ( $56.1 \text{ Tg N yr}^{-1}$ ) and 2012-2014 ( $58.5 \text{ Tg N yr}^{-1}$ ) due  
13 to the opposing changes in different regions. Total  $\text{NO}_y$  deposition was lowest in 2006 ( $50.5$   
14  $\text{Tg N}$ ), and peaked at  $60.8 \text{ Tg N}$  in 2012. Since then, it appears that global  $\text{NO}_y$  deposition  
15 may be on the decline. Future observations in the coming years will be needed to establish  
16 whether this most recent decline is robust or temporary.

17 Figure 7 shows the calculated long-term trends in the measured wet  $\text{NO}_3^-$  deposition for  
18 locations across North America, Europe, and East Asia where at least 15 years of quality-  
19 controlled annual data are available (the coverage of these observation is the same as in  
20 Figure 4). The observations over North America show the gradient in trend from negligible in  
21 the west to steeply and significantly decreasing in northeastern US and southeastern Canada.  
22 The steepest observed statistically significant trend ( $-0.18 \text{ kg N ha}^{-1} \text{ yr}^{-2}$ ) occurs east of  
23 Detroit in southwestern Ontario, Canada. In Europe, only one of the gridded observations has  
24 a statistically significant trend ( $-0.07 \text{ kg N ha}^{-1} \text{ yr}^{-2}$ ), located near the border of Denmark and  
25 Germany. The other locations in Europe show statistically insignificant trends over the long-  
26 term. In East Asia, we also we find that most of the stations record statistically negligible  
27 trends over the long term (only two of the 11 gridded observations have significant trends).  
28 The steepest observed trend in this region ( $+0.39 \text{ kg N ha}^{-1} \text{ yr}^{-2}$ ) is found near Kuala Lumpur  
29 and is statistically significant.

30 We compare the long-term trends in these measurements with our satellite-constrained  
31 trends in wet  $\text{NO}_3^-$  deposition. We find a similar spatial gradient in North America, and the  
32 same magnitude of declines through the northeast US and southern Ontario ( $-0.12$  to  $-0.16 \text{ kg}$

1 N ha<sup>-1</sup> yr<sup>-2</sup>). Over Europe, our estimates have low statistical significance in the trends  
2 throughout much of this region, consistent with the observations. Where we do see statistical  
3 significance (northern United Kingdom, southern Denmark, and in some central/eastern  
4 European countries), observations are not available over the long-term for evaluation. In East  
5 Asia, our satellite-constrained ~~estimated~~ trends estimates show statistically significant  
6 increases throughout much of the region (in contrast to most of the available observations).  
7 The trend over Kuala Lumpur is significant and positive (+0.24 kg N ha<sup>-1</sup> yr<sup>-2</sup>) as expected  
8 from the available measurements.

9 We again emphasize the small sample size in Europe (N = 16) and East Asia (N = 11).  
10 Moreover, in many cases trends in one (or both) datasets are small and/or insignificant. For  
11 these reasons, we focus on comparing the confidence intervals of the measured and satellite-  
12 constrained trends. We find that for 129 of the 136 gridded pairs (> 90% of the data), the 95%  
13 confidence intervals overlap; of the pairs for which the intervals do not overlap, 3 (out of 109)  
14 occur in North America, 1 (out of 16) in Europe, and 3 (out of 11) in East Asia. For a large  
15 majority of the data in all three regions we therefore conclude that the satellite-derived trends  
16 are not significantly different from the trends inferred with ground-based measurements.  
17 Continued long-term measurements with better spatial coverage are imperative to better  
18 evaluate long-term estimates of global NO<sub>y</sub> deposition especially throughout Europe and East  
19 Asia (but also in other parts of the world where long-term coverage is not available at all).

### 20 **3.3 Changes in Continental Export of NO<sub>y</sub>**

21 NO<sub>y</sub> deposition is a transboundary, and even intercontinental, issue (HTAP, 2010). In a  
22 multi-model study, Sanderson et al. (2008) found that between 3-10% of NO<sub>x</sub> emissions from  
23 Europe, North America, South Asia, and East Asia are ultimately deposited over foreign  
24 regions. Long range transport events of NO<sub>2</sub> alone can be systematically detected by satellite  
25 observations (Zien et al., 2014). Here we extend such studies using our satellite-constrained  
26 long-term estimates of annual NO<sub>y</sub> deposition to evaluate how the amount of NO<sub>x</sub> exported  
27 from specific regions (i.e. the net balance between emissions and deposition over a land area)  
28 has changed over the last two decades.

29 Decreases in NO<sub>y</sub> export over the Atlantic Ocean from North America and increases in  
30 export over the western Pacific Ocean from East Asia are evident in Figure 5. We find that net  
31 export of NO<sub>x</sub> from North America via atmospheric transport has decreased by more than

1 40% (from 2.5 Tg N yr<sup>-1</sup> in 1996, to 1.4 Tg N yr<sup>-1</sup> in 2014). In contrast, we find that export of  
2 NO<sub>x</sub> from Asia increased by 40% from 3.3 Tg N in 1996, to a maximum of 4.7 Tg N in 2011,  
3 with a subsequent decrease to 3.8 Tg N by 2014. As a result of these opposing trends, total  
4 deposition to the global oceans has changed remarkably little (25.0 Tg N yr<sup>-1</sup> in 1996-1998  
5 compared to 24.4 Tg N yr<sup>-1</sup> in 2012-2014), but has experienced substantial regional  
6 redistribution.

7 NO<sub>y</sub> export from North America has received considerable attention. Urban plumes  
8 from the eastern US that are transported across the North Atlantic for several days could still  
9 contain 20-50 ppb of reactive nitrogen oxides (Neuman et al. 2006). A recent detailed GEOS-  
10 Chem study of nitrogen deposition over the US estimated that net annual export of NO<sub>x</sub> was  
11 around 38% of NO<sub>x</sub> emissions (or 2.5 Tg N) for 2006-2008 (Zhang et al. 2012). We estimate  
12 a similar fraction of export from the continental US using our observationally-constrained  
13 simulation (34% ± 2% from 1996-2014), with a small decreasing trend from 35% in 1996-  
14 1998 to 32% in 2012-2014. As a result of declining emissions we find that absolute export  
15 from the continental US decreased by 50% from 2.9 Tg N in 1996 to 1.5 Tg N in 2014. We  
16 find declines in NO<sub>y</sub> deposition across the Atlantic Ocean, with small though statistically  
17 significant declines as far downwind as southern Greenland. The decreases downwind of the  
18 continent are clearest and most significant in the winter, spring, and fall (Fig. 5b, c, and e)  
19 while the trends are more local in the summer (when the NO<sub>x</sub> lifetime is short and when  
20 midlatitude wind speeds are weaker).

21 We similarly calculate the net imbalance between NO<sub>x</sub> emissions and NO<sub>y</sub> deposition  
22 over western European countries and find a decrease of almost 40%, from 2.2 Tg N to 1.3 Tg  
23 N. We calculate mean export of NO<sub>x</sub> emissions from western European countries to be 45% ±  
24 4%, with a notable decreasing trend from 50% in 1996-1998 to 40% in 2012-2014.~~In contrast~~  
25 ~~to the continental US, we also find a notable decrease in the fraction of emissions that are~~  
26 ~~exported from western European countries (from 50% in 1996-1998 to 40% in 2012-2014).~~  
27 As a result, the decrease in net export is steeper than the decrease in emissions from the  
28 region. As alluded to in Section 3.2, the decrease in NO<sub>x</sub> export from some western European  
29 countries has likely compensated for increases in emissions in some of the central/eastern  
30 European countries, and in western Russia, where we find dry deposition has significantly  
31 increased, but wet deposition has decreased or shows no significant net trend.

1 Reactive nitrogen transport from Asia has previously been shown to contribute to O<sub>x</sub>  
2 production across the mid-latitude Pacific reaching as far as the west coast of North America  
3 (Walker et al., 2010; Zhang et al., 2008), and major NO<sub>x</sub> transport events from China can be  
4 indirectly observed by NO<sub>2</sub> columns (Lee et al., 2014). Our satellite-constrained estimate  
5 predicts that export from China alone ~~(24% ± 4% of emissions)~~ more than tripled from 1.0 Tg  
6 N in 1996 to a maximum of 3.5 Tg N in 2011, then decreased to 2.5 Tg N by 2014. We  
7 estimate that an average of 24% ± 4% emissions from China are exported, varying over time  
8 from as little as 15% of emissions in 1998 to a maximum of 31% of emissions in 2011 (with  
9 an overall increasing trend). Zhao et al. (2017) used a higher resolution (0.5° x 0.667°)  
10 GEOS-Chem simulation and estimated that 36% of China's NO<sub>x</sub> emissions over 2008-2012  
11 are exported. We calculate an export fraction of around 27% for the same time period. The  
12 discrepancy between the two estimates may be attributed to the coarser horizontal resolution  
13 of our simulation (2° x 2.5°), pointing to important resolution-dependent effects in global  
14 simulations of deposition. Other factors may include the use of different NO<sub>x</sub> emissions (our  
15 satellite-constrained emissions indicate rapid change over this period of time), and the  
16 treatment of adjacent oceans.

17 Zhao et al. (2015) used GEOS-Chem to explore nitrogen deposition to the  
18 northwestern Pacific Ocean off the coast of China from 2008-2010. They estimated total (wet  
19 + dry) NO<sub>y</sub> deposition of 6.9 kg N ha<sup>-1</sup> yr<sup>-1</sup> and 3.1 kg N ha<sup>-1</sup> yr<sup>-1</sup> to the Yellow Sea and the  
20 South China Sea respectively. Our simulation predicts that NO<sub>y</sub> deposition to the same  
21 regions of the Yellow Sea increased from 5.1 kg N ha<sup>-1</sup> yr<sup>-1</sup> in 1996 to 9.5 kg N ha<sup>-1</sup> yr<sup>-1</sup> by  
22 2012 and to the South China Sea from 2.8 kg N ha<sup>-1</sup> yr<sup>-1</sup> in 1996 to 4.3 kg N ha<sup>-1</sup> yr<sup>-1</sup> in 2011.  
23 Subsequent declines in the following years will hopefully have encouraging implications for  
24 nitrogen availability and the incidence of algal blooms in these regions (Hu et al., 2010).

25 Export of pollution from China has been shown to influence deposition over Japan in  
26 particular (e.g. Lin et al., 2008). Using observations of wet nitrate deposition, Morino et al.  
27 (2011) report increases throughout Japan from 1989-2008, and attribute this trend largely to  
28 transport from China. Likewise, integrated NO<sub>y</sub> deposition over Japan increased (p < 0.01) in  
29 our satellite-constrained estimate. In fact, we find that Japan transitioned from a net  
30 “exporter” of NO<sub>y</sub> over 1996-2006 (emissions exceeded local deposition by up to 24%) to a  
31 net “importer” of NO<sub>y</sub> over 2007-2014 (local deposition exceeded emissions by up to 20%).  
32 The increase in deposition was dominated by statistically significant increases in wet

1 deposition in some parts of the country. We find the increase over Japan is most uniform  
2 during the spring (Fig. 5, MAM), consistent with transport from China being pronounced  
3 during the spring season (Tanimoto et al., 2005). Nevertheless, the impacts of local  $\text{NO}_x$   
4 controls can also be important. Dry deposition dominates the decline in annual  $\text{NO}_y$   
5 deposition just west of Tokyo. Declines are seen throughout the southern part of the country  
6 during both the summer and fall seasons (Fig. 5, JJA and SON). These results demonstrate the  
7 indirect relationship between local emissions and local deposition of  $\text{NO}_y$  for regions  
8 influenced by atmospheric transport, and also show how long-term trends can depend strongly  
9 on the season and process (wet or dry deposition).

### 10 **3.4 Sensitivity of $\text{NO}_y$ Deposition to $\text{NH}_3$ Emissions**

11 The transport and ultimate deposition of oxidized nitrogen may be tightly coupled with  
12 the reduced nitrogen ( $\text{NH}_x = \text{NH}_3 + \text{NH}_4^+$ ) and sulfate systems, due to the formation of  
13  $\text{NH}_4\text{NO}_3$  aerosol that becomes favorable once all  $\text{H}_2\text{SO}_4$  has been neutralized (i.e., if there is  
14 “excess”  $\text{NH}_3$ ). Examples of the resulting non-linearity between  $\text{PM}_{2.5}$  concentrations and  
15 precursor emissions have been noted in the literature (Banzhaf et al., 2013; Derwent et al.,  
16 2009; Fowler et al., 2005). The formation of  $\text{NH}_4\text{NO}_3$  aerosol at the expense of  $\text{HNO}_3$  with  
17 changing excess ammonia could therefore conceivably change the atmospheric lifetime of  
18  $\text{NO}_y$  at the surface; accumulation mode aerosol may have a dry deposition lifetime of days  
19 whereas  $\text{HNO}_3$  tends to have a dry deposition lifetime of shorter than a day. As a result, the  
20 predicted footprint of source impacts is sensitive to  $\text{NH}_3$  emissions (Lee et al., 2016).

21 Contemporary emissions of  $\text{NH}_3$  are highly uncertain (Reis et al., 2009), so we perform  
22 a sensitivity experiment by perturbing (increasing) all anthropogenic and natural  $\text{NH}_3$   
23 emissions everywhere in the model by 25% for the year 2012. Predicted  $\text{NO}_y$  deposition from  
24 this simulation is compared to the predicted  $\text{NO}_y$  deposition in the 2012 simulation where  
25  $\text{NH}_3$  emissions were not perturbed. Since we have not altered the emissions of oxidized  
26 nitrogen, simple mass balance dictates that increases in deposition over some regions will be  
27 countered by decreases elsewhere. Our perturbation is therefore to be interpreted as an  
28 experiment that tests how accurately the spatial pattern in  $\text{NO}_y$  deposition at our model  
29 resolution can be predicted, given some uncertainty in  $\text{NH}_3$  emissions. Given the horizontal  
30 resolution of our simulation ( $2.5^\circ \times 2.0^\circ$ ), we acknowledge that our estimates of the sensitivity



1 of  $\text{NO}_y$  deposition to perturbations in  $\text{NH}_3$  emissions may underestimate the importance of  
2 those interactions at finer spatial scales.

3 Figure 8 shows the results of this experiment. The sensitivity of  $\text{NO}_y$  deposition to an  
4 increase in  $\text{NH}_3$  emissions is positive or negative depending on the region, while net  
5 deposition over the global domain does not change (to within 1-2%). Over the continents, the  
6 sensitivity in total (wet + dry)  $\text{NO}_y$  deposition to the 25% perturbation in  $\text{NH}_3$  emissions tends  
7 to be less than  $\pm 5\%$ , with a few exceptions. We find differences in  $\text{NO}_y$  deposition on the  
8 order of 10% over parts of high-latitude Russia, northwest and central Africa, eastern China,  
9 southern South America, and Australia. However, with the exception of China, these are also  
10 regions where deposition is relatively low. We conclude that for most regions of interest, our  
11 satellite-constrained estimates of  $\text{NO}_y$  deposition over the continents and their trends will not  
12 be severely impacted by uncertainty in the  $\text{NH}_3$  inventories.

13 Notably, the difference exceeds +50% over Myanmar, suggesting that simulated  $\text{NO}_y$   
14 deposition over this country is extremely sensitive to changes in  $\text{NH}_3$  emissions. It is clear  
15 from Figure 8 that this results from a high sensitivity in dry deposition (middle panel) instead  
16 of wet deposition (bottom panel). Myanmar has some of the lowest estimated  $\text{NH}_3$  emissions  
17 in all of South and East Asia (at least an order of magnitude lower than surrounding India,  
18 China, and Thailand), so this sensitivity reflects changes in the upwind emissions and  
19 subsequent transport of  $\text{NO}_y$ . We find the opposite sensitivity in nearby Cambodia, where the  
20 sensitivity of dry  $\text{NO}_y$  deposition to a 25% perturbation in  $\text{NH}_3$  emissions is -50%.

21 Over the oceans, the sensitivity of  $\text{NO}_y$  deposition to the 25% increase in  $\text{NH}_3$  emissions  
22 is generally low ( $< \pm 5\%$ ), with the expected exceptions in areas that are directly offshore  
23 from major continental source regions. In the North Atlantic Ocean east of Canada and  
24 Greenland, and in the North Pacific Ocean off the coasts of China, Japan and in the South  
25 China Sea, the sensitivity of  $\text{NO}_y$  deposition is between 5-20%. Our predicted decrease in dry  
26  $\text{NO}_y$  deposition to the Yellow Sea given an increase in  $\text{NH}_3$  emissions is consistent with  
27 previous adjoint analyses showing increased  $\text{NO}_y$  dry deposition in this region with a decrease  
28 in Asian  $\text{NH}_3$  emissions (Zhao et al. 2015). Likewise, the sensitivity of deposition to the  
29 Mediterranean Sea is between 10-20%. The differences in  $\text{NO}_y$  deposition over the oceans  
30 results from sensitivity in both dry and wet deposition (although in the case of the  
31 Mediterranean it is dominated by dry deposition). We conclude that although changes (or  
32 uncertainties) in  $\text{NH}_3$  emissions can impact the distance of transport and deposition to oceans

1 downwind of the major NO<sub>x</sub> sources, the absolute magnitude of deposition is low where the  
2 sensitivity of NO<sub>y</sub> deposition to NH<sub>3</sub> is relatively high.

### 3 **3.5 Other Considerations**

4 A number of other uncertainties are important in an inversion of satellite NO<sub>2</sub> columns  
5 to calculate surface NO<sub>x</sub> emissions and simulate of long-term NO<sub>y</sub> deposition. These can  
6 depend on, for example, the choice of inversion approach, errors in the satellite retrieval, and  
7 uncertainties in model processes (e.g. emissions, boundary layer mixing, chemical NO<sub>x</sub> sinks,  
8 meteorology, and dry deposition).

9 Cooper et al. (2017) found that the finite mass balance inversion approach used here can  
10 be improved upon by using an iterative method that performs with similar accuracy as a four-  
11 dimensional variational data assimilation. Multi-constituent data assimilation also shows  
12 considerable promise for constraints on surface NO<sub>x</sub> emissions (Myazaki et al. 2017). Satellite  
13 retrieval algorithms continue to develop with advances that will improve the accuracy of  
14 future estimates of satellite-constrained NO<sub>y</sub> deposition.

15 Uncertainties in model processes are also of interest. For example, uncertainties in the  
16 chemical sink of NO<sub>x</sub> alone (e.g. the rate of HNO<sub>3</sub> formation, heterogeneous loss of N<sub>2</sub>O<sub>5</sub>  
17 onto aerosol) can have a substantial impact on top-down emissions estimates (Stavrakou et  
18 al., 2013), suggesting more fundamental work in constraining these processes is required. Lin  
19 et al. (2010) found that top-down NO<sub>x</sub> emissions estimates over East Asia are sensitive to  
20 other model uncertainties including planetary boundary layer mixing scheme, lightning  
21 emissions, diurnal profile of emissions, and a-priori NO<sub>x</sub>, CO, and VOC emissions.  
22 Uncertainties in model meteorology are also important. For example, the MERRA  
23 precipitation fields used in our study are known to correlate weakly with observational  
24 datasets (Rienecker et al., 2011), but improvements can be expected from MERRA-2 due to  
25 the inclusion of gauge- and satellite-based precipitation corrections (Reichle et al., 2017).  
26 Finally, dry deposition schemes are also highly variable among models (Flechard et al., 2011;  
27 Hardacre et al., 2015), and future work in dry deposition evaluation should be a priority.

28 Nonetheless, despite these uncertainties we find a high degree of consistency between  
29 observations and our predictions in the long-term changes to deposition. Evidence continues  
30 to emerge about potential biases in bottom-up inventories (e.g. Travis et al. 2016), and our  
31 observational constraint on NO<sub>x</sub> emissions mitigates against such biases. We expect

1 continued advancements in inversion approaches, satellite retrieval algorithms, and  
2 fundamental atmospheric chemistry processes will allow for increasingly accurate satellite-  
3 based constraints on deposition.

#### 5 **4 Conclusion**

6 NO<sub>y</sub> deposition represents about half of the total reactive nitrogen deposited to Earth's  
7 surface. Even in the US where nitrogen oxide emissions have decreased substantially,  
8 constituents of NO<sub>y</sub> remain major contributors to the nitrogen deposited in areas of concern  
9 (Lee et al. 2016; Li et al. 2016). We applied NO<sub>2</sub> observations from multiple satellites over  
10 1996-2014 together with the GEOS-Chem chemical transport model to estimate long-term  
11 changes to reactive nitrogen oxide deposition around the world. Given the effective global  
12 mass balance between NO<sub>x</sub> emissions and deposition of reactive nitrogen oxides, we show  
13 that satellite constraints on NO<sub>x</sub> emissions can provide a powerful top-down constraint on  
14 deposition in order to evaluate long-term changes worldwide. Observations from the GOME,  
15 SCIAMACHY, and GOME-2 satellite instruments have provided continuous global coverage  
16 over the last 20 years, allowing observational constraints on NO<sub>y</sub> deposition that enhance the  
17 poor spatial coverage of ground-based deposition measurements.

18 We find substantial variability in regional trends of NO<sub>y</sub> deposition. NO<sub>y</sub> deposition  
19 declined most steeply throughout the northeastern United States at a rate of ~~by~~ up to -0.6 kg N  
20 ha<sup>-1</sup> yr<sup>-2</sup>, but has also decreased significantly throughout most of the country and in southern  
21 Canada. In Europe, statistically significant declines at a rate of up to -0.1 kg N ha<sup>-1</sup> yr<sup>-2</sup> are  
22 seen over some western countries. On the other hand, NO<sub>y</sub> deposition has increased  
23 substantially throughout East Asia, exceeding a rate of +0.6 kg N ha<sup>-1</sup> yr<sup>-2</sup> in some parts.  
24 Since reductions in deposition over some regions were counteracted by increases in others,  
25 global NO<sub>y</sub> deposition did not change considerably over the long term. However, we find that  
26 global NO<sub>y</sub> deposition could now be on the decline overall, since deposition in Asia peaked  
27 around 2010-2012. The ability to resolve the striking recent decline in NO<sub>y</sub> deposition in  
28 China (despite prior projections of increasing NO<sub>x</sub> emissions) demonstrates one of the  
29 attributes of using a satellite-based constraint. Future observations will be important in  
30 evaluating whether this trend persists.

31 We find that changes over the last two decades in the export of reactive nitrogen oxides  
32 via atmospheric transport have impacted countries downwind of source regions. Export from

1 North America has decreased by at least 40%, while export from Asia has increased by the  
2 same relative amount. We find evidence that decreases in  $\text{NO}_x$  export from some western  
3 European countries have counteracted increases in local emissions from some eastern/central  
4 European countries, resulting in negligible net change in  $\text{NO}_y$  deposition over the long term.  
5 Likewise, Japan is highly sensitive to changes in export from China, but this depends strongly  
6 on the season and whether wet and dry deposition are both considered. While uncertainty in  
7  $\text{NH}_3$  emissions can impact the footprint of  $\text{NO}_y$  export and deposition, we show that this  
8 sensitivity is small in most regions of concern.

9 Direct measurements of deposition are sparse, inhibiting evaluation. This is especially  
10 challenging for global simulations, where individual measurements may not necessarily be  
11 regionally representative. Nevertheless, we find that for the vast majority of locations our  
12 satellite-derived trends are largely consistent with the observed trends. Expanded coverage of  
13 ground-based observations over the long-term is needed to more comprehensively evaluate  
14 long-term estimates of global  $\text{NO}_y$  deposition. This need also motivates the value of using  
15 alternative observational constraints like the satellite  $\text{NO}_2$  columns as presented here.

16 Forthcoming satellite observations of  $\text{NO}_2$  at higher spatial resolution (e.g. TROPOMI  
17 (Veefkind et al., 2012)) and with diurnally varying observations (e.g. TEMPO (Zoogman et  
18 al., 2017), Sentinel-4, and GEMS) will offer increasingly robust constraints on  $\text{NO}_x$  emissions  
19 that affect  $\text{NO}_y$  deposition. Satellite observations of  $\text{NH}_3$  (e.g. Van Damme et al., 2014) may  
20 offer additional opportunities to constrain the reactive nitrogen budget. Higher resolution  
21 global modeling will also be an important development to accurately account for non-linear  
22  $\text{NO}_2$  losses in global emission inversions (Valin et al., 2011).

23 Our satellite-constrained estimates of  $\text{NO}_y$  document interannual changes over the past  
24 two decades worldwide. We expect that this information will be useful in future research into  
25 the impacts of nitrogen deposition to important biodiversity hotspots, in regions dealing with  
26 excessive nitrogen inputs leading to algal blooms, or estimating the changing impacts of  
27 nitrogen deposition on global carbon uptake.

28

## 29 **Appendix 1**

30 We simulate atmospheric chemistry from 1996 to 2014 using the GEOS-Chem  
31 chemical transport model ([www.geos-chem.org](http://www.geos-chem.org)) v9-02. Our simulations are driven with the

1 MERRA meteorological product at a global horizontal resolution of  $2.5^\circ \times 2.0^\circ$  and 47  
2 vertical layers. GEOS-Chem includes detailed  $\text{HO}_x$ - $\text{NO}_x$ -VOC- $\text{O}_3$ -aerosol chemistry (Bey et  
3 al. 2001; Park et al. 2004), with isoprene chemistry following Paulot et al. (2009a, 2009b) and  
4 gas-aerosol partitioning for the sulfate-nitrate-ammonium system calculated according to the  
5 ISORROPIA II equilibrium model (Fountoukis and Nenes, 2007). Gas-aerosol phase coupling  
6 occurs via  $\text{N}_2\text{O}_5$  uptake (Evans and Jacob, 2005) and  $\text{HO}_2$  uptake (Mao et al., 2013) in  
7 addition to other heterogeneous chemistry (Jacob, 2000) and aerosol effects on photolysis  
8 frequencies (Martin et al., 2003). Our simulations use timesteps of 15 minutes for transport  
9 and convection, and 30 minutes for emissions and chemistry.

10 Removal by wet deposition occurs through scavenging in moist convective updrafts, as  
11 well as in-cloud and below-cloud scavenging during large-scale precipitation for water-  
12 soluble aerosol and gases (Amos et al., 2012; Liu et al., 2001). Removal by dry deposition is  
13 calculated based on the widely used resistance-in-series formulation from Wesely (1989),  
14 described for GEOS-Chem in Wang et al. (1998) and Zhang et al. (2001) for aerosol. Dry  
15 deposition of  $\text{NO}_y$  over the United States was recently explored and evaluated in detail by  
16 Zhang et al. (2012).

17 Anthropogenic emissions are prescribed by the NEI 2005 inventory for the United  
18 States (<http://www.epa.gov/ttnchie1/trends/>), the CAC inventory for Canada  
19 (<http://www.ec.gc.ca/pdb/cac/>), the BRAVO inventory for Mexico (Kuhns et al., 2005), the  
20 EMEP inventory for Europe (<http://www.emep.int/>), and Zhang et al. (2009) for China and  
21 Southeast Asia. Elsewhere, the EDGAR v3 emission inventory is used for anthropogenic  
22  $\text{NO}_x$ , CO, and  $\text{SO}_x$  (Olivier et al., 2005), the GEIA inventory for  $\text{NH}_3$  (Bouwman et al., 1997),  
23 and the RETRO inventory for VOCs (Hu et al., 2015). Monthly scaling of  $\text{NO}_x$  emissions is  
24 included in North America (based on the VISTAS inventory), Europe (based on the EMEP  
25 inventory), and Asia (based on the Zhang et al. (2009) inventory). Monthly scaling of  
26 EDGAR emissions is based on the seasonality from the Global Emission Inventory Activity  
27 (Benkovitz et al 1996). Aircraft emissions are from the AEIC inventory (Stettler et al., 2011).  
28 Scale factors based on energy statistics following van Donkelaar et al. (2008) are used to scale  
29  $\text{NO}_x$ , CO and  $\text{SO}_x$  emissions between 1996 and 2010 for years when the emissions are  
30 unavailable from the inventory. For other species and for emissions beyond 2010, the closest  
31 available year is used. Biogenic VOC emissions are calculated using the MEGAN model  
32 (Guenther et al., 2006). Biomass burning emissions are according to the GFED3 inventory

1 (Mu et al., 2011). Soil NO<sub>x</sub> is calculated using the Berkeley-Dalhousie Parameterization  
2 (Hudman et al., 2012). Lightning NO<sub>x</sub> is implemented according to Murray et al. (2012).  
3 These a-priori surface NO<sub>x</sub> emissions are overwritten by our satellite-derived top-down  
4 estimates in the assessment of NO<sub>y</sub> deposition.

5

6

## 7 **Acknowledgements**

8 This work was supported by NSERC and Environment and Climate Change Canada. We  
9 acknowledge the free use of tropospheric NO<sub>2</sub> column data from the GOME, SCIAMACHY,  
10 and GOME-2 sensors from [www.temis.nl](http://www.temis.nl). We further acknowledge the NADP, CAPMoN,  
11 EMEP and EANET regional monitoring networks, and the World Data Centre for  
12 Precipitation Chemistry for access to wet deposition data.

13

## 1 **References**

- 2 van der A, R. J., Eskes, H. J., Boersma, K. F., van Noije, T. P. C., Van Roozendaal, M., De  
3 Smedt, I., Peters, D. H. M. U. and Meijer, E. W.: Trends, seasonal variability and dominant  
4 NO<sub>x</sub> source derived from a ten year record of NO<sub>2</sub> measured from space, *J. Geophys. Res.*,  
5 113(D4), D04302, doi:10.1029/2007JD009021, 2008.
- 6 Amos, H. M., Jacob, D. J., Holmes, C. D., Fisher, J. A., Wang, Q., Yantosca, R. M., Corbitt,  
7 E. S., Galarneau, E., Rutter, A. P., Gustin, M. S., Steffen, A., Schauer, J. J., Graydon, J. A.,  
8 Louis, V. L. St., Talbot, R. W., Edgerton, E. S., Zhang, Y. and Sunderland, E. M.: Gas-  
9 particle partitioning of atmospheric Hg(II) and its effect on global mercury deposition, *Atmos.*  
10 *Chem. Phys.*, 12(1), 591–603, doi:10.5194/acp-12-591-2012, 2012.
- 11 Banzhaf, S., Schaap, M., Wichink Kruit, R. J., Denier van der Gon, H. A. C., Stern, R. and  
12 Builtjes, P. J. H.: Impact of emission changes on secondary inorganic aerosol episodes across  
13 Germany, *Atmos. Chem. Phys.*, 13(23), 11675–11693, doi:10.5194/acp-13-11675-2013,  
14 2013.
- 15 Beirle, S., Huntrieser, H. and Wagner, T.: Direct satellite observation of lightning-produced  
16 NO<sub>x</sub>, *Atmos. Chem. Phys.*, 10(22), 10965–10986, doi:10.5194/acp-10-10965-2010, 2010.
- 17 Bey, I., Jacob, D. J., Yantosca, R. M., Logan, J. A., Field, B. D., Fiore, A. M., Li, Q., Liu, H.  
18 Y., Mickley, L. J. and Schultz, M. G.: Global modeling of tropospheric chemistry with  
19 assimilated meteorology: Model description and evaluation, *J. Geophys. Res.*, 106(D19),  
20 23073, doi:10.1029/2001JD000807, 2001.
- 21 Bobbink, R., Hicks, K., Galloway, J., Spranger, T., Alkemade, R., Ashmore, M., Bustamante,  
22 M., Cinderby, S., Davidson, E., Dentener, F., Emmett, B., Erisman, J.-W., Fenn, M., Gilliam,  
23 F., Nordin, A., Pardo, L. and De Vries, W.: Global assessment of nitrogen deposition effects  
24 on terrestrial plant diversity: a synthesis, *Ecol. Appl.*, 20(1), 30–59, doi:10.1890/08-1140.1,  
25 2010.
- 26 Boersma, K. F., Eskes, H. J. and Brinksma, E. J.: Error analysis for tropospheric NO<sub>2</sub>  
27 retrieval from space, *J. Geophys. Res.*, 109(D4), D04311–D04311,  
28 doi:10.1029/2003JD003962, 2004.
- 29 Boersma, K. F., Vinken, G. C. M. and Eskes, H. J.: Representativeness errors in comparing  
30 chemistry transport and chemistry climate models with satellite UV–Vis tropospheric column

1 retrievals, *Geosci. Model Dev.*, 9(2), 875–898, doi:10.5194/gmd-9-875-2016, 2016.

2 Bouwman, A. F., Lee, D. S., Asman, W. A. H., Dentener, F. J., Van Der Hoek, K. W. and  
3 Olivier, J. G. J.: A global high-resolution emission inventory for ammonia, *Global*  
4 *Biogeochem. Cycles*, 11(4), 561–587, doi:10.1029/97GB02266, 1997.

5 Bouwman, A. F., Van Vuuren, D. P., Derwent, R. G. and Posch, M.: A Global Analysis of  
6 Acidification and Eutrophication of Terrestrial Ecosystems, *Water. Air. Soil Pollut.*, 141(1/4),  
7 349–382, doi:10.1023/A:1021398008726, 2002.

8 Castellanos, P. and Boersma, K. F.: Reductions in nitrogen oxides over Europe driven by  
9 environmental policy and economic recession., *Sci. Rep.*, 2, 265, doi:10.1038/srep00265,  
10 2012.

11 Cheng, M., Jiang, H., Guo, Z., Zhang, X. and Lu, X.: Estimating NO<sub>2</sub> dry deposition using  
12 satellite data in eastern China, *Int. J. Remote Sens.*, 34(7), 2548–2565,  
13 doi:10.1080/01431161.2012.747019, 2013.

14 Cooper, M., Martin, R. V., Padmanabhan, A. and Henze, D. K.: Comparing mass balance and  
15 adjoint methods for inverse modeling of nitrogen dioxide columns for global nitrogen oxide  
16 emissions, *J. Geophys. Res. Atmos.*, 122(8), 4718–4734, doi:10.1002/2016JD025985, 2017.

17 Van Damme, M., Clarisse, L., Heald, C. L., Hurtmans, D., Ngadi, Y., Clerbaux, C., Dolman,  
18 A. J., Erisman, J. W. and Coheur, P. F.: Global distributions, time series and error  
19 characterization of atmospheric ammonia (NH<sub>3</sub>) from IASI satellite observations, *Atmos.*  
20 *Chem. Phys.*, 14(6), 2905–2922, doi:10.5194/ACP-14-2905-2014, 2014.

21 Dentener, F., Drevet, J., Lamarque, J. F., Bey, I., Eickhout, B., Fiore, A. M., Hauglustaine, D.,  
22 Horowitz, L. W., Krol, M., Kulshrestha, U. C., Lawrence, M., Galy-Lacaux, C., Rast, S.,  
23 Shindell, D., Stevenson, D., Van Noije, T., Atherton, C., Bell, N., Bergman, D., Butler, T.,  
24 Cofala, J., Collins, B., Doherty, R., Ellingsen, K., Galloway, J., Gauss, M., Montanaro, V.,  
25 Müller, J. F., Pitari, G., Rodriguez, J., Sanderson, M., Solmon, F., Strahan, S., Schultz, M.,  
26 Sudo, K., Szopa, S. and Wild, O.: Nitrogen and sulfur deposition on regional and global  
27 scales: A multimodel evaluation, *Global Biogeochem. Cycles*, 20(4), n/a-n/a,  
28 doi:10.1029/2005GB002672, 2006.

29 Derwent, R., Witham, C., Redington, A., Jenkin, M., Stedman, J., Yardley, R. and Hayman,  
30 G.: Particulate matter at a rural location in southern England during 2006: Model sensitivities  
31 to precursor emissions, *Atmos. Environ.*, 43(3), 689–696,



1 doi:10.1016/j.atmosenv.2008.09.077, 2009.

2 Dietze, M. C. and Moorcroft, P. R.: Tree mortality in the eastern and central United States:  
3 patterns and drivers, *Glob. Chang. Biol.*, 17(11), 3312–3326, doi:10.1111/j.1365-  
4 2486.2011.02477.x, 2011.

5 van Donkelaar, A., Martin, R. V., Leaitch, W. R., Macdonald, A. M., Walker, T. W., Streets,  
6 D. G., Zhang, Q., Dunlea, E. J., Jimenez, J. L., Dibb, J. E., Huey, L. G., Weber, R. and  
7 Andreae, M. O.: Analysis of aircraft and satellite measurements from the Intercontinental  
8 Chemical Transport Experiment (INTEX-B) to quantify long-range transport of East Asian  
9 sulfur to Canada, *Atmos. Chem. Phys.*, 8(11), 2999–3014, doi:10.5194/acp-8-2999-2008,  
10 2008.

11 Duce, R. A., LaRoche, J., Altieri, K., Arrigo, K. R., Baker, A. R., Capone, D. G., Cornell, S.,  
12 Dentener, F., Galloway, J., Ganeshram, R. S., Geider, R. J., Jickells, T., Kuypers, M. M.,  
13 Langlois, R., Liss, P. S., Liu, S. M., Middelburg, J. J., Moore, C. M., Nickovic, S., Oschlies,  
14 A., Pedersen, T., Prospero, J., Schlitzer, R., Seitzinger, S., Sorensen, L. L., Uematsu, M.,  
15 Ulloa, O., Voss, M., Ward, B. and Zamora, L.: Impacts of atmospheric anthropogenic  
16 nitrogen on the open ocean., *Science*, 320(5878), 893–7, doi:10.1126/science.1150369, 2008.

17 Duncan, B. N., Yoshida, Y., de Foy, B., Lamsal, L. N., Streets, D. G., Lu, Z., Pickering, K. E.  
18 and Krotkov, N. A.: The observed response of Ozone Monitoring Instrument (OMI) NO<sub>2</sub>  
19 columns to NO<sub>x</sub> emission controls on power plants in the United States: 2005–2011, *Atmos.*  
20 *Environ.*, 81, 102–111, doi:10.1016/j.atmosenv.2013.08.068, 2013.

21 Ellis, R. A., Jacob, D. J., Sulprizio, M. P., Zhang, L., Holmes, C. D., Schichtel, B. A., Blett,  
22 T., Porter, E., Pardo, L. H. and Lynch, J. A.: Present and future nitrogen deposition to national  
23 parks in the United States: critical load exceedances, *Atmos. Chem. Phys.*, 13(17), 9083–  
24 9095, doi:10.5194/acp-13-9083-2013, 2013.

25 Evans, M. J. and Jacob, D. J.: Impact of new laboratory studies of N<sub>2</sub>O<sub>5</sub> hydrolysis on  
26 global model budgets of tropospheric nitrogen oxides, ozone, and OH, *Geophys. Res. Lett.*,  
27 32(9), L09813, doi:10.1029/2005GL022469, 2005.

28 Flechard, C. R., Nemitz, E., Smith, R. I., Fowler, D., Vermeulen, A. T., Bleeker, A., Erisman,  
29 J. W., Simpson, D., Zhang, L., Tang, Y. S. and Sutton, M. A.: Dry deposition of reactive  
30 nitrogen to European ecosystems: a comparison of inferential models across the NitroEurope  
31 network, *Atmos. Chem. Phys.*, 11(6), 2703–2728, doi:10.5194/acp-11-2703-2011, 2011.

1 Fountoukis, C. and Nenes, A.: ISORROPIA II: a computationally efficient thermodynamic  
2 equilibrium model for  $\text{K}^+$ - $\text{Ca}^{2+}$ - $\text{Mg}^{2+}$ - $\text{NH}_4^+$ - $\text{Na}^+$ - $\text{SO}_4^{2-}$ - $\text{NO}_3^-$ - $\text{Cl}^-$ - $\text{H}_2\text{O}$  aerosols,  
3 *Atmos. Chem. Phys.*, 7(17), 4639–4659, 2007.

4 Fowler, D., Muller, J., Smith, R. I., Cape, J. N. and Erisman, J. W.: Nonlinearities in source  
5 receptor relationships for sulfur and nitrogen compounds., *Ambio*, 34(1), 41–6, 2005.

6 de Foy, B., Lu, Z. and Streets, D. G.: Satellite  $\text{NO}_2$  retrievals suggest China has exceeded its  
7  $\text{NO}_x$  reduction goals from the twelfth Five-Year Plan, *Sci. Rep.*, 6, doi:10.1038/srep35912,  
8 2016.

9 Galloway, J. N., Dentener, F. J., Capone, D. G., Boyer, E. W., Howarth, R. W., Seitzinger, S.  
10 P., Asner, G. P., Cleveland, C. C., Green, P. A., Holland, E. A., Karl, D. M., Michaels, A. F.,  
11 Porter, J. H., Townsend, A. R. and Vorosmarty, C. J.: Nitrogen cycles: past, present, and  
12 future, *Biogeochemistry*, 70(2), 153–226, 2004.

13 Galloway, J. N., Townsend, A. R., Erisman, J. W., Bekunda, M., Cai, Z., Freney, J. R.,  
14 Martinelli, L. A., Seitzinger, S. P. and Sutton, M. A.: Transformation of the Nitrogen Cycle:  
15 Recent Trends, Questions, and Potential Solutions, *Science* (80-. ), 320(5878), 2008.

16 Geddes, J. A., Martin, R. V., Boys, B. L. and van Donkelaar, A.: Long-Term Trends  
17 Worldwide in Ambient  $\text{NO}_2$  Concentrations Inferred from Satellite Observations, *Environ.*  
18 *Health Perspect.*, 124(3), doi:10.1289/ehp.1409567, 2015.

19 Guenther, A., Karl, T., Harley, P., Wiedinmyer, C., Palmer, P. I. and Geron, C.: Estimates of  
20 global terrestrial isoprene emissions using MEGAN (Model of Emissions of Gases and  
21 Aerosols from Nature), *Atmos. Chem. Phys.*, 6, 3181–3210, 2006.

22 Hardacre, C., Wild, O. and Emberson, L.: An evaluation of ozone dry deposition in global  
23 scale chemistry climate models, *Atmos. Chem. Phys.*, 15(11), 6419–6436, doi:10.5194/acp-  
24 15-6419-2015, 2015.

25 Hernández, D. L., Vallano, D. M., Zavaleta, E. S., Tzankova, Z., Pasari, J. R., Weiss, S.,  
26 Selmants, P. C. and Morozumi, C.: Nitrogen Pollution Is Linked to US Listed Species  
27 Declines, *Bioscience*, 66(3), 213–222, doi:10.1093/biosci/biw003, 2016.

28 Hilboll, A., Richter, A. and Burrows, J. P.: Long-term changes of tropospheric  $\text{NO}_2$  over  
29 megacities derived from multiple satellite instruments, *Atmos. Chem. Phys.*, 13(8), 4145–  
30 4169, doi:10.5194/acp-13-4145-2013, 2013.

- 1 Holland, E. A., Braswell, B. H., Sulzman, J. and Lamarque, J. F.: Nitrogen deposition onto  
2 the United States and western Europe: Synthesis of observations and models, *Ecol. Appl.*,  
3 15(1), 38–57, doi:10.1890/03-5162, 2005.
- 4 HTAP: Hemispheric Transport of Air Pollution 2010 - Part A: Ozone and Particulate Matter,  
5 New York. [online] Available from: <http://www.htap.org/>, 2010.
- 6 Hu, C., Li, D., Chen, C., Ge, J., Muller-Karger, F. E., Liu, J., Yu, F. and He, M.-X.: On the  
7 recurrent *Ulva prolifera* blooms in the Yellow Sea and East China Sea, *J. Geophys. Res.*,  
8 115(C5), C05017, doi:10.1029/2009JC005561, 2010.
- 9 Hu, L., Millet, D. B., Baasandorj, M., Griffis, T. J., Travis, K. R., Tessum, C. W., Marshall, J.  
10 D., Reinhart, W. F., Mikoviny, T., Müller, M., Wisthaler, A., Graus, M., Warneke, C. and de  
11 Gouw, J.: Emissions of C6 -C8 aromatic compounds in the United States: Constraints from  
12 tall tower and aircraft measurements, *J. Geophys. Res. Atmos.*, 120(2), 826–842,  
13 doi:10.1002/2014JD022627, 2015.
- 14 Hudman, R. C., Moore, N. E., Mebust, A. K., Martin, R. V, Russell, A. R., Valin, L. C. and  
15 Cohen, R. C.: Steps towards a mechanistic model of global soil nitric oxide emissions:  
16 implementation and space based-constraints, *Atmos. Chem. Phys.*, 12(16), 7779–7795,  
17 doi:10.5194/acp-12-7779-2012, 2012.
- 18 Isbell, F., Reich, P. B., Tilman, D., Hobbie, S. E., Polasky, S. and Binder, S.: Nutrient  
19 enrichment, biodiversity loss, and consequent declines in ecosystem productivity., *Proc. Natl.*  
20 *Acad. Sci. U. S. A.*, 110(29), 11911–6, doi:10.1073/pnas.1310880110, 2013.
- 21 Jacob, D. J.: Heterogeneous chemistry and tropospheric ozone, *Atmos. Environ.*, 34(12),  
22 2131–2159, doi:10.1016/S1352-2310(99)00462-8, 2000.
- 23 Jaegle, L., Steinberger, L., Martin, R. V and Chance, K.: Global partitioning of NO<sub>x</sub> sources  
24 using satellite observations: Relative roles of fossil fuel combustion, biomass burning and soil  
25 emissions, *Faraday Discuss.*, 130, 407–423, doi:10.1039/b502128f, 2005.
- 26 Jia, Y., Yu, G., Gao, Y., He, N., Wang, Q., Jiao, C. and Zuo, Y.: Global inorganic nitrogen  
27 dry deposition inferred from ground- and space-based measurements., *Sci. Rep.*, 6, 19810,  
28 doi:10.1038/srep19810, 2016.
- 29 Kanakidou, M., Myriokefalitakis, S., Daskalakis, N., Fanourgakis, G., Nenes, A., Baker, A.  
30 R., Tsigaridis, K., Mihalopoulos, N., Kanakidou, M., Myriokefalitakis, S., Daskalakis, N.,

1 Fanourgakis, G., Nenes, A., Baker, A. R., Tsigaridis, K. and Mihalopoulos, N.: Past, Present,  
2 and Future Atmospheric Nitrogen Deposition, *J. Atmos. Sci.*, 73(5), 2039–2047,  
3 doi:10.1175/JAS-D-15-0278.1, 2016.

4 Kendall, M. G.: Rank Correlation Methods, 4th ed., Charles Griffen, London., 1975.

5 Konovalov, I. B., Beekmann, M., Burrows, J. P. and Richter, A.: Satellite measurement based  
6 estimates of decadal changes in European nitrogen oxides emissions, *Atmos. Chem. Phys.*,  
7 8(10), 2623–2641, doi:10.5194/acp-8-2623-2008, 2008.

8 Konovalov, I. B., Beekmann, M., Richter, A., Burrows, J. P. and Hilboll, A.: Multi-annual  
9 changes of NO<sub>x</sub> emissions in megacity regions: nonlinear trend analysis of satellite  
10 measurement based estimates, *Atmos. Chem. Phys.*, 10(17), 8481–8498, doi:10.5194/acp-10-  
11 8481-2010, 2010a.

12 Konovalov, I. B., Beekmann, M., Richter, A., Burrows, J. P. and Hilboll, A.: Multi-annual  
13 changes of NO<sub>x</sub> emissions in megacity regions: nonlinear trend analysis of satellite  
14 measurement based estimates, *Atmos. Chem. Phys.*, 10(17), 8481–8498, doi:10.5194/acp-10-  
15 8481-2010, 2010b.

16 Krotkov, N. A., McLinden, C. A., Li, C., Lamsal, L. N., Celarier, E. A., Marchenko, S. V.,  
17 Swartz, W. H., Bucsela, E. J., Joiner, J., Duncan, B. N., Folkert Boersma, K., Pepijn  
18 Veefkind, J., Levelt, P. F., Fioletov, V. E., Dickerson, R. R., He, H., Lu, Z. and Streets, D. G.:  
19 Aura OMI observations of regional SO<sub>2</sub> and NO<sub>2</sub> pollution changes from 2005 to 2015,  
20 *Atmos. Chem. Phys.*, 16(7), 4605–4629, doi:10.5194/acp-16-4605-2016, 2016.

21 Kuhns, H., Knipping, E. M. and Vukovich, J. M.: Development of a United States-Mexico  
22 Emissions Inventory for the Big Bend Regional Aerosol and Visibility Observational  
23 (BRAVO) Study., *J. Air Waste Manag. Assoc.*, 55(5), 677–92, 2005.

24 Lamarque, J.-F., Dentener, F., McConnell, J., Ro, C.-U., Shaw, M., Vet, R., Bergmann, D.,  
25 Cameron-Smith, P., Dalsoren, S., Doherty, R., Faluvegi, G., Ghan, S. J., Josse, B., Lee, Y. H.,  
26 MacKenzie, I. A., Plummer, D., Shindell, D. T., Skeie, R. B., Stevenson, D. S., Strode, S.,  
27 Zeng, G., Curran, M., Dahl-Jensen, D., Das, S., Fritzsche, D. and Nolan, M.: Multi-model  
28 mean nitrogen and sulfur deposition from the Atmospheric Chemistry and Climate Model  
29 Intercomparison Project (ACCMIP): evaluation of historical and projected future changes,  
30 *Atmos. Chem. Phys.*, 13(16), 7997–8018, doi:10.5194/acp-13-7997-2013, 2013.

31 Lamsal, L. N., Martin, R. V., van Donkelaar, A., Celarier, E. A., Bucsela, E. J., Boersma, K.

1 F., Dirksen, R., Luo, C. and Wang, Y.: Indirect validation of tropospheric nitrogen dioxide  
2 retrieved from the OMI satellite instrument: Insight into the seasonal variation of nitrogen  
3 oxides at northern midlatitudes, *J. Geophys. Res.*, 115(D5), D05302,  
4 doi:10.1029/2009JD013351, 2010.

5 Lamsal, L. N., Martin, R. V., Padmanabhan, A., Van Donkelaar, A., Zhang, Q., Sioris, C. E.,  
6 Chance, K., Kurosu, T. P. and Newchurch, M. J.: Application of satellite observations for  
7 timely updates to global anthropogenic NO<sub>x</sub> emission inventories, *Geophys. Res. Lett.*, 38(5),  
8 2011.

9 Lee, H.-J., Kim, S.-W., Brioude, J., Cooper, O. R., Frost, G. J., Kim, C.-H., Park, R. J.,  
10 Trainer, M. and Woo, J.-H.: Transport of NO<sub>x</sub> in East Asia identified by satellite and in situ  
11 measurements and Lagrangian particle dispersion model simulations, *J. Geophys. Res.*  
12 *Atmos.*, 119(5), 2574–2596, doi:10.1002/2013JD021185, 2014.

13 Lee, H.-M., Paulot, F., Henze, D. K., Travis, K., Jacob, D. J., Pardo, L. H. and Schichtel, B.  
14 A.: Sources of nitrogen deposition in Federal Class I areas in the US, *Atmos. Chem. Phys.*,  
15 16(2), 525–540, doi:10.5194/acp-16-525-2016, 2016.

16 Li, Y., Schichtel, B. A., Walker, J. T., Schwede, D. B., Chen, X., Lehmann, C. M. B.,  
17 Puchalski, M. A., Gay, D. A. and Collett, J. L.: Increasing importance of deposition of  
18 reduced nitrogen in the United States., *Proc. Natl. Acad. Sci. U. S. A.*, 113(21), 5874–9,  
19 doi:10.1073/pnas.1525736113, 2016.

20 Lin, J.-T., McElroy, M. B. and Boersma, K. F.: Constraint of anthropogenic NO<sub>x</sub> emissions in  
21 China from different sectors: a new methodology using multiple satellite retrievals, *Atmos.*  
22 *Chem. Phys.*, 10(1), 63–78, doi:10.5194/acp-10-63-2010, 2010.

23 Lin, M., Oki, T., Bengtsson, M., Kanae, S., Holloway, T. and Streets, D. G.: Long-range  
24 transport of acidifying substances in East Asia—Part II: Source–receptor relationships,  
25 *Atmos. Environ.*, 42(24), 5956–5967, doi:10.1016/j.atmosenv.2008.03.039, 2008.

26 Liu, H., Jacob, D. J., Bey, I. and Yantosca, R. M.: Constraints from <sup>210</sup>Pb and <sup>7</sup>Be on wet  
27 deposition and transport in a global three-dimensional chemical tracer model driven by  
28 assimilated meteorological fields, *J. Geophys. Res. Atmos.*, 106(D11), 12109–12128,  
29 doi:10.1029/2000JD900839, 2001.

30 Liu, L. L. and Greaver, T. L.: A review of nitrogen enrichment effects on three biogenic  
31 GHGs: the CO<sub>2</sub> sink may be largely offset by stimulated N<sub>2</sub>O and CH<sub>4</sub> emission, *Ecol. Lett.*,

1 12(10), 1103–1117, 2009.

2 Lu, X., Jiang, H., Zhang, X., Liu, J., Zhang, Z., Jin, J., Wang, Y., Xu, J. and Cheng, M.:  
3 Estimated global nitrogen deposition using NO<sub>2</sub> column density, *Int. J. Remote Sens.*, 34(24),  
4 8893–8906, doi:10.1080/01431161.2013.853894, 2013.

5 Lu, Z., Streets, D. G., De Foy, B., Lamsal, L. N., Duncan, B. N. and Xing, J.: Emissions of  
6 nitrogen oxides from US urban areas: Estimation from Ozone Monitoring Instrument  
7 retrievals for 2005-2014, *Atmos. Chem. Phys.*, 15(18), 10367–10383, doi:10.5194/acp-15-  
8 10367-2015, 2015.

9 Mann, H. B.: Non-parametric tests against trend, *Econometrica*, 13, 163–171, 1945.

10 Mao, J., Fan, S., Jacob, D. J. and Travis, K. R.: Radical loss in the atmosphere from Cu-Fe  
11 redox coupling in aerosols, *Atmos. Chem. Phys.*, 13(2), 509–519, doi:10.5194/acp-13-509-  
12 2013, 2013.

13 Martin, R. V.: Global inventory of nitrogen oxide emissions constrained by space-based  
14 observations of NO<sub>2</sub> columns, *J. Geophys. Res.*, 108(D17), 4537,  
15 doi:10.1029/2003JD003453, 2003.

16 Martin, R. V., Jacob, D. J., Yantosca, R. M., Chin, M. and Ginoux, P.: Global and regional  
17 decreases in tropospheric oxidants from photochemical effects of aerosols, *J. Geophys. Res.*  
18 *Atmos.*, 108(D3), n/a-n/a, doi:10.1029/2002JD002622, 2003.

19 McLinden, C. A., Fioletov, V., Boersma, K. F., Krotkov, N., Sioris, C. E., Veefkind, J. P. and  
20 Yang, K.: Air quality over the Canadian oil sands: A first assessment using satellite  
21 observations, *Geophys. Res. Lett.*, 39(4), n/a-n/a, doi:10.1029/2011GL050273, 2012.

22 Mijling, B., van der A, R. J. and Zhang, Q.: Regional nitrogen oxides emission trends in East  
23 Asia observed from space, *Atmos. Chem. Phys.*, 13(23), 12003–12012, doi:10.5194/acp-13-  
24 12003-2013, 2013.

25 Miyazaki, K., Eskes, H., Sudo, K., Boersma, K. F., Bowman, K. and Kanaya, Y.: Decadal  
26 changes in global surface NO<sub>x</sub> emissions from multi-constituent satellite data assimilation,  
27 *Atmos. Chem. Phys. Discuss.*, 1–48, doi:10.5194/acp-2016-529, 2016.

28 Morino, Y., Ohara, T., Kurokawa, J., Kuribayashi, M., Uno, I. and Hara, H.: Temporal  
29 variations of nitrogen wet deposition across Japan from 1989 to 2008, *J. Geophys. Res.*,  
30 116(D6), D06307, doi:10.1029/2010JD015205, 2011.

1 Mu, M., Randerson, J. T., van der Werf, G. R., Giglio, L., Kasibhatla, P., Morton, D., Collatz,  
2 G. J., DeFries, R. S., Hyer, E. J., Prins, E. M., Griffith, D. W. T., Wunch, D., Toon, G. C.,  
3 Sherlock, V. and Wennberg, P. O.: Daily and 3-hourly variability in global fire emissions and  
4 consequences for atmospheric model predictions of carbon monoxide, *J. Geophys. Res.*  
5 *Atmos.*, 116(D24), n/a-n/a, doi:10.1029/2011JD016245, 2011.

6 Murray, L. T., Jacob, D. J., Logan, J. A., Hudman, R. C. and Koshak, W. J.: Optimized  
7 regional and interannual variability of lightning in a global chemical transport model  
8 constrained by LIS/OTD satellite data, *J. Geophys. Res. Atmos.*, 117(D20), n/a-n/a,  
9 doi:10.1029/2012JD017934, 2012.

10 Neuman, J. A., Parrish, D. D., Trainer, M., Ryerson, T. B., Holloway, J. S., Nowak, J. B.,  
11 Swanson, A., Flocke, F., Roberts, J. M., Brown, S. S., Stark, H., Sommariva, R., Stohl, A.,  
12 Peltier, R., Weber, R., Wollny, A. G., Sueper, D. T., Hubler, G. and Fehsenfeld, F. C.:  
13 Reactive nitrogen transport and photochemistry in urban plumes over the North Atlantic  
14 Ocean, *J. Geophys. Res. Atmos.*, 111(D23), doi:10.1029/2005JD007010, 2006.

15 Nowlan, C. R., Martin, R. V., Philip, S., Lamsal, L. N., Krotkov, N. A., Marais, E. A., Wang,  
16 S. and Zhang, Q.: Global dry deposition of nitrogen dioxide and sulfur dioxide inferred from  
17 space-based measurements, *Global Biogeochem. Cycles*, n/a-n/a,  
18 doi:10.1002/2014GB004805, 2014.

19 Olivier, J. G. J., Van Aardenne, J. A., Dentener, F. J., Pagliari, V., Ganzeveld, L. N. and  
20 Peters, J. A. H. W.: Recent trends in global greenhouse gas emissions: regional trends 1970–  
21 2000 and spatial distribution of key sources in 2000, *Environ. Sci.*, 2(2–3), 81–99,  
22 doi:10.1080/15693430500400345, 2005.

23 Park, R. J., Jacob, D. J., Field, B. D. and Yantosca, R. M.: Natural and transboundary  
24 pollution influences on sulfate-nitrate-ammonium aerosols in the United States: Implications  
25 for policy, *J. Geophys. Res.*, 109(D15), D15204, doi:10.1029/2003JD004473, 2004.

26 Paulot, F., Crouse, J. D., Kjaergaard, H. G., Kroll, J. H., Seinfeld, J. H. and Wennberg, P. O.:  
27 Isoprene photooxidation: new insights into the production of acids and organic nitrates,  
28 *Atmos. Chem. Phys.*, 9(4), 1479–1501, 2009a.

29 Paulot, F., Crouse, J. D., Kjaergaard, H. G., Kürten, A., St Clair, J. M., Seinfeld, J. H. and  
30 Wennberg, P. O.: Unexpected epoxide formation in the gas-phase photooxidation of  
31 isoprene., *Science*, 325(5941), 730–3, doi:10.1126/science.1172910, 2009b.

- 1 Reay, D. S., Dentener, F., Smith, P., Grace, J. and Feely, R. A.: Global nitrogen deposition  
2 and carbon sinks, *Nat. Geosci.*, 1(7), 430–437, 2008.
- 3 Reichle, R. H., Draper, C. S., Liu, Q., Girotto, M., Mahanama, S. P. P., Koster, R. D., De  
4 Lannoy, G. J. M., Reichle, R. H., Draper, C. S., Liu, Q., Girotto, M., Mahanama, S. P. P.,  
5 Koster, R. D. and Lannoy, G. J. M. De: Assessment of MERRA-2 Land Surface Hydrology  
6 Estimates, *J. Clim.*, 30(8), 2937–2960, doi:10.1175/JCLI-D-16-0720.1, 2017.
- 7 Reis, S., Pinder, R. W., Zhang, M., Lijie, G. and Sutton, M. A.: Reactive nitrogen in  
8 atmospheric emission inventories, *Atmos. Chem. Phys.*, 9(19), 7657–7677, doi:10.5194/acp-  
9 9-7657-2009, 2009.
- 10 Richter, A., Eyring, V., Burrows, J. P., Bovensmann, H., Lauer, A., Sierk, B. and Crutzen, P.  
11 J.: Satellite measurements of NO<sub>2</sub> from international shipping emissions, *Geophys. Res.*  
12 *Let.*, 31(23), doi:10.1029/2004GL020822, 2004.
- 13 Richter, A., Burrows, J. P., Nüss, H., Granier, C. and Niemeier, U.: Increase in tropospheric  
14 nitrogen dioxide over China observed from space., *Nature*, 437(7055), 129–32,  
15 doi:10.1038/nature04092, 2005.
- 16 Rienecker, M. M., Suarez, M. J., Gelaro, R., Todling, R., Bacmeister, J., Liu, E., Bosilovich,  
17 M. G., Schubert, S. D., Takacs, L., Kim, G.-K., Bloom, S., Chen, J., Collins, D., Conaty, A.,  
18 da Silva, A., Gu, W., Joiner, J., Koster, R. D., Lucchesi, R., Molod, A., Owens, T., Pawson,  
19 S., Pegion, P., Redder, C. R., Reichle, R., Robertson, F. R., Ruddick, A. G., Sienkiewicz, M.,  
20 Woollen, J., Rienecker, M. M., Suarez, M. J., Gelaro, R., Todling, R., Julio Bacmeister, Liu,  
21 E., Bosilovich, M. G., Schubert, S. D., Takacs, L., Kim, G.-K., Bloom, S., Chen, J., Collins,  
22 D., Conaty, A., Silva, A. da, Gu, W., Joiner, J., Koster, R. D., Lucchesi, R., Molod, A.,  
23 Owens, T., Pawson, S., Pegion, P., Redder, C. R., Reichle, R., Robertson, F. R., Ruddick, A.  
24 G., Sienkiewicz, M. and Woollen, J.: MERRA: NASA's Modern-Era Retrospective Analysis  
25 for Research and Applications, *J. Clim.*, 24(14), 3624–3648, doi:10.1175/JCLI-D-11-00015.1,  
26 2011.
- 27 Russell, A. R., Valin, L. C. and Cohen, R. C.: Trends in OMI NO<sub>2</sub> observations over the  
28 United States: effects of emission control technology and the economic recession, *Atmos.*  
29 *Chem. Phys.*, 12(24), 12197–12209, doi:10.5194/acp-12-12197-2012, 2012.
- 30 Sanderson, M. G., Dentener, F. J., Fiore, A. M., Cuvelier, C., Keating, T. J., Zuber, A.,  
31 Atherton, C. S., Bergmann, D. J., Diehl, T., Doherty, R. M., Duncan, B. N., Hess, P.,



1 Horowitz, L. W., Jacob, D. J., Jonson, J. E., Kaminski, J. W., Lupu, A., MacKenzie, I. A.,  
2 Mancini, E., Marmer, E., Park, R., Pitari, G., Prather, M. J., Pringle, K. J., Schroeder, S.,  
3 Schultz, M. G., Shindell, D. T., Szopa, S., Wild, O. and Wind, P.: A multi-model study of the  
4 hemispheric transport and deposition of oxidised nitrogen, *Geophys. Res. Lett.*, 35(17), 2008.

5 De Schrijver, A., De Frenne, P., Ampoorter, E., Van Nevel, L., Demey, A., Wuyts, K. and  
6 Verheyen, K.: Cumulative nitrogen input drives species loss in terrestrial ecosystems, *Glob.*  
7 *Ecol. Biogeogr.*, 20(6), 803–816, doi:10.1111/j.1466-8238.2011.00652.x, 2011.

8 Sen, P. K.: Estimates of the Regression Coefficient Based on Kendall's Tau, *J. Am. Stat.*  
9 *Assoc.*, 63(324), 1379–1389, doi:10.1080/01621459.1968.10480934, 1968.

10 Sickles II, J. E. and Shadwick, D. S.: Changes in air quality and atmospheric deposition in the  
11 eastern United States: 1990–2004, *J. Geophys. Res.*, 112(D17), D17301,  
12 doi:10.1029/2006JD007843, 2007.

13 Sickles II, J. E. and Shadwick, D. S.: Air quality and atmospheric deposition in the eastern  
14 US: 20 years of change, *Atmos. Chem. Phys.*, 15(1), 173–197, doi:10.5194/acp-15-173-2015,  
15 2015.

16 Souri, A. H., Choi, Y., Jeon, W., Li, X., Pan, S., Diao, L. and Westenbarger, D. A.:  
17 Constraining NO<sub>x</sub> emissions using satellite NO<sub>2</sub> measurements during 2013 DISCOVER-AQ  
18 Texas campaign, *Atmos. Environ.*, 131, 371–381, doi:10.1016/j.atmosenv.2016.02.020, 2016.

19 Stavrou, T., Müller, J.-F., Boersma, K. F., De Smedt, I. and van der A, R. J.: Assessing the  
20 distribution and growth rates of NO<sub>x</sub> emission sources by inverting a 10-year record of NO<sub>2</sub>  
21 satellite columns, *Geophys. Res. Lett.*, 35(10), L10801, doi:10.1029/2008GL033521, 2008.

22 Stavrou, T., Müller, J.-F., Boersma, K. F., van der A, R. J., Kurokawa, J., Ohara, T. and  
23 Zhang, Q.: Key chemical NO<sub>x</sub> sink uncertainties and how they influence top-down emissions  
24 of nitrogen oxides, *Atmos. Chem. Phys.*, 13(17), 9057–9082, doi:10.5194/acp-13-9057-2013,  
25 2013.

26 Stettler, M. E. J., Eastham, S. and Barrett, S. R. H.: Air quality and public health impacts of  
27 UK airports. Part I: Emissions, *Atmos. Environ.*, 45(31), 5415–5424,  
28 doi:10.1016/j.atmosenv.2011.07.012, 2011.

29 Streets, D. G., Canty, T., Carmichael, G. R., de Foy, B., Dickerson, R. R., Duncan, B. N.,  
30 Edwards, D. P., Haynes, J. A., Henze, D. K., Houyoux, M. R., Jacob, D. J., Krotkov, N. A.,

1 Lamsal, L. N., Liu, Y., Lu, Z., Martin, R. V., Pfister, G. G., Pinder, R. W., Salawitch, R. J.  
2 and Wecht, K. J.: Emissions estimation from satellite retrievals: A review of current  
3 capability, *Atmos. Environ.*, 77, 1011–1042, doi:10.1016/j.atmosenv.2013.05.051, 2013.

4 Tanimoto, H., Sawa, Y., Matsueda, H., Uno, I., Ohara, T., Yamaji, K., Kurokawa, J. and  
5 Yonemura, S.: Significant latitudinal gradient in the surface ozone spring maximum over East  
6 Asia, *Geophys. Res. Lett.*, 32(21), L21805, doi:10.1029/2005GL023514, 2005.

7 Templer, P. H., Pinder, R. W. and Goodale, C. L.: Effects of nitrogen deposition on  
8 greenhouse-gas fluxes for forests and grasslands of North America, *Front. Ecol. Environ.*,  
9 10(10), 547–553, doi:10.1890/120055, 2012.

10 Travis, K. R., Jacob, D. J., Fisher, J. A., Kim, P. S., Marais, E. A., Zhu, L., Yu, K., Miller, C.  
11 C., Yantosca, R. M., Sulprizio, M. P., Thompson, A. M., Wennberg, P. O., Crounse, J. D., St.  
12 Clair, J. M., Cohen, R. C., Laughner, J. L., Dibb, J. E., Hall, S. R., Ullmann, K., Wolfe, G.  
13 M., Pollack, I. B., Peischl, J., Neuman, J. A. and Zhou, X.: Why do models overestimate  
14 surface ozone in the Southeast United States?, *Atmos. Chem. Phys.*, 16(21), 13561–13577,  
15 doi:10.5194/acp-16-13561-2016, 2016.

16 Valin, L. C., Russell, a. R., Hudman, R. C. and Cohen, R. C.: Effects of model resolution on  
17 the interpretation of satellite NO<sub>2</sub> observations, *Atmos. Chem. Phys.*, 11(22), 11647–11655,  
18 doi:10.5194/acp-11-11647-2011, 2011.

19 Veefkind, J. P., Aben, I., McMullan, K., Förster, H., de Vries, J., Otter, G., Claas, J., Eskes,  
20 H. J., de Haan, J. F., Kleipool, Q., van Weele, M., Hasekamp, O., Hoogeveen, R., Landgraf,  
21 J., Snel, R., Tol, P., Ingmann, P., Voors, R., Kruizinga, B., Vink, R., Visser, H. and Levelt, P.  
22 F.: TROPOMI on the ESA Sentinel-5 Precursor: A GMES mission for global observations of  
23 the atmospheric composition for climate, air quality and ozone layer applications, *Remote*  
24 *Sens. Environ.*, 120, 70–83, doi:10.1016/j.rse.2011.09.027, 2012.

25 Vet, R., Artz, R. S., Carou, S., Shaw, M., Ro, C.-U., Aas, W., Baker, A., Bowersox, V. C.,  
26 Dentener, F., Galy-Lacaux, C., Hou, A., Pienaar, J. J., Gillett, R., Forti, M. C., Gromov, S.,  
27 Hara, H., Khodzher, T., Mahowald, N. M., Nickovic, S., Rao, P. S. P. and Reid, N. W.: A  
28 global assessment of precipitation chemistry and deposition of sulfur, nitrogen, sea salt, base  
29 cations, organic acids, acidity and pH, and phosphorus, *Atmos. Environ.*, 93, 3–100,  
30 doi:10.1016/j.atmosenv.2013.10.060, 2014.

31 Vinken, G. C. M., Boersma, K. F., Maasackers, J. D., Adon, M. and Martin, R. V.:

1 Worldwide biogenic soil NO<sub>x</sub> emissions inferred from OMI NO<sub>2</sub> observations, *Atmos.*  
2 *Chem. Phys. Discuss.*, 14(10), 14683–14724, doi:10.5194/acpd-14-14683-2014, 2014.

3 Walker, T. W., Martin, R. V., van Donkelaar, A., Leaitch, W. R., MacDonald, A. M., Anlauf,  
4 K. G., Cohen, R. C., Bertram, T. H., Huey, L. G., Avery, M. A., Weinheimer, A. J., Flocke, F.  
5 M., Tarasick, D. W., Thompson, A. M., Streets, D. G. and Liu, X.: Trans-Pacific transport of  
6 reactive nitrogen and ozone to Canada during spring, *Atmos. Chem. Phys.*, 10(17), 8353–  
7 8372, doi:10.5194/acp-10-8353-2010, 2010.

8 Wang, Y. H., Jacob, D. J. and Logan, J. A.: Global simulation of tropospheric O<sub>3</sub>-NO<sub>x</sub>-  
9 hydrocarbon chemistry 1. Model formulation, *J. Geophys. Res.*, 103(D9), 10713–10725,  
10 doi:10.1029/98JD00158, 1998.

11 Wesely, M. L.: Parameterization of surface resistances to gaseous dry deposition in regional-  
12 scale numerical models, *Atmos. Environ.*, 23(6), 1293–1304, doi:10.1016/0004-  
13 6981(89)90153-4, 1989.

14 World Health Organization: WHO Air Quality Guidelines for Europe, 2nd edition, [online]  
15 Available from: [http://www.euro.who.int/en/publications/abstracts/air-quality-guidelines-for-](http://www.euro.who.int/en/publications/abstracts/air-quality-guidelines-for-europe)  
16 europe (Accessed 28 October 2016), 2000.

17 Zbieranowski, A. L. and Aherne, J.: Long-term trends in atmospheric reactive nitrogen across  
18 Canada: 1988–2007, *Atmos. Environ.*, 45(32), 5853–5862,  
19 doi:10.1016/j.atmosenv.2011.06.080, 2011.

20 Zhang, L., Gong, S., Padro, J. and Barrie, L.: A size-segregated particle dry deposition  
21 scheme for an atmospheric aerosol module, *Atmos. Environ.*, 35(3), 549–560,  
22 doi:10.1016/S1352-2310(00)00326-5, 2001.

23 Zhang, L., Jacob, D. J., Boersma, K. F., Jaffe, D. A., Olson, J. R., Bowman, K. W., Worden,  
24 J. R., Thompson, A. M., Avery, M. A., Cohen, R. C., Dibb, J. E., Flock, F. M., Fuelberg, H.  
25 E., Huey, L. G., McMillan, W. W., Singh, H. B. and Weinheimer, A. J.: Transpacific  
26 transport of ozone pollution and the effect of recent Asian emission increases on air quality in  
27 North America: an integrated analysis using satellite, aircraft, ozonesonde, and surface  
28 observations, *Atmos. Chem. Phys.*, 8(20), 6117–6136, doi:10.5194/acp-8-6117-2008, 2008.

29 Zhang, L., Jacob, D. J., Knipping, E. M., Kumar, N., Munger, J. W., Carouge, C. C., Van  
30 Donkelaar, A., Wang, Y. X. and Chen, D.: Nitrogen deposition to the United States:  
31 Distribution, sources, and processes, *Atmos. Chem. Phys.*, 12(10), 4539–4554, 2012.

1 Zhang, Q., Streets, D. G., He, K., Wang, Y., Richter, A., Burrows, J. P., Uno, I., Jang, C. J.,  
2 Chen, D., Yao, Z. and Lei, Y.: NO<sub>x</sub> emission trends for China, 1995–2004: The view from  
3 the ground and the view from space, *J. Geophys. Res.*, 112(D22), D22306,  
4 doi:10.1029/2007JD008684, 2007.

5 Zhang, Q., Streets, D. G., Carmichael, G. R., He, K. B., Huo, H., Kannari, A., Klimont, Z.,  
6 Park, I. S., Reddy, S., Fu, J. S., Chen, D., Duan, L., Lei, Y., Wang, L. T. and Yao, Z. L.:  
7 Asian emissions in 2006 for the NASA INTEX-B mission, *Atmos. Chem. Phys.*, 9(14), 5131–  
8 5153, doi:10.5194/acp-9-5131-2009, 2009.

9 Zhao, Y., Zhang, L., Pan, Y., Wang, Y., Paulot, F. and Henze, D. K.: Atmospheric nitrogen  
10 deposition to the northwestern Pacific: seasonal variation and source attribution, *Atmos.*  
11 *Chem. Phys.*, 15(18), 10905–10924, doi:10.5194/acp-15-10905-2015, 2015.

12 Zhao, Y., Zhang, L., Chen, Y., Liu, X., Xu, W., Pan, Y. and Duan, L.: Atmospheric nitrogen  
13 deposition to China: A model analysis on nitrogen budget and critical load exceedance,  
14 *Atmos. Environ.*, 153, 32–40, doi:10.1016/j.atmosenv.2017.01.018, 2017.

15 Zien, A. W., Richter, A., Hilboll, A., Blechschmidt, A.-M. and Burrows, J. P.: Systematic  
16 analysis of tropospheric NO<sub>2</sub> long-range transport events detected in GOME-2 satellite data,  
17 *Atmos. Chem. Phys.*, 14(14), 7367–7396, doi:10.5194/acp-14-7367-2014, 2014.

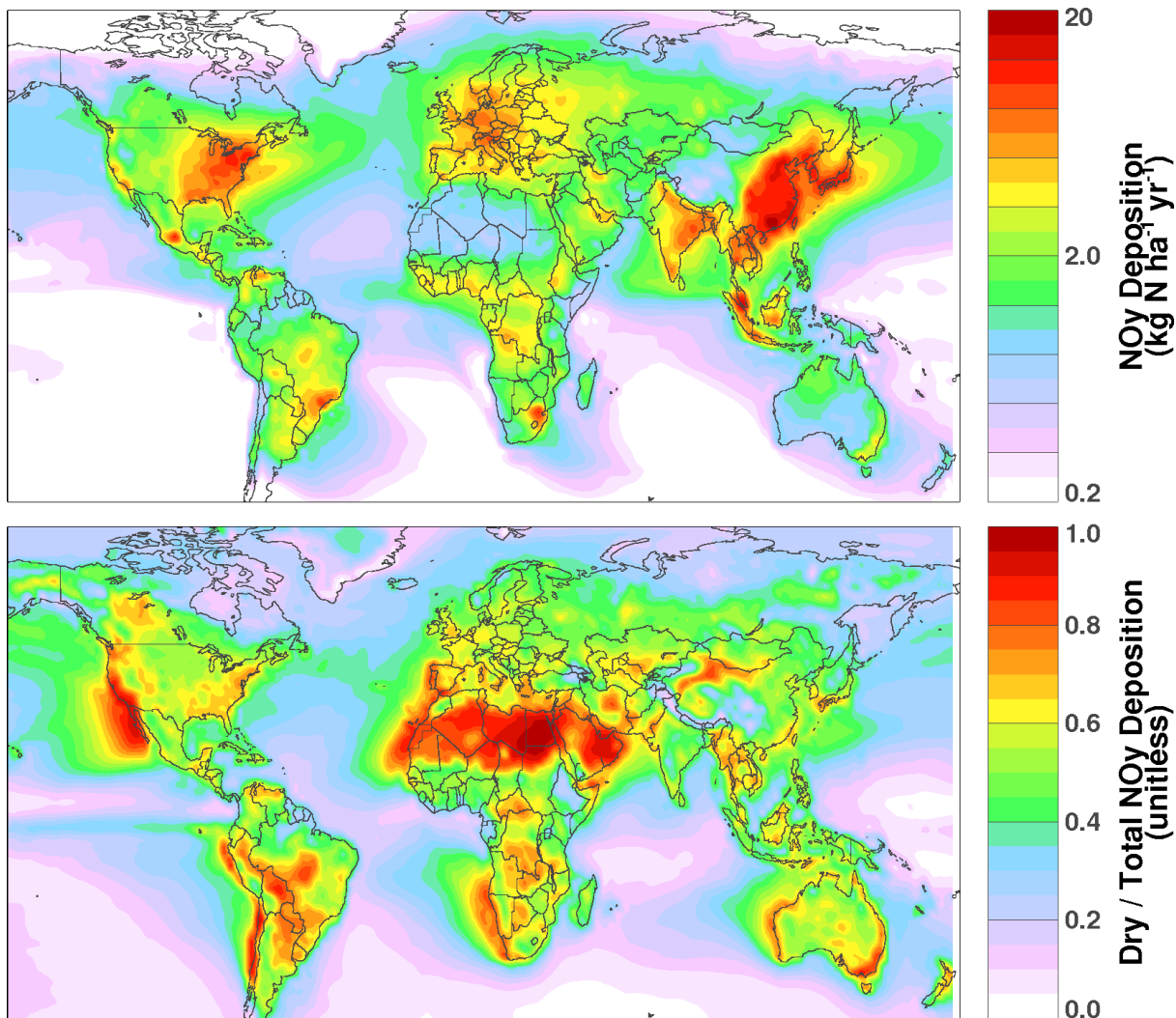
18 Zoogman, P., Liu, X., Suleiman, R. M., Pennington, W. F., Flittner, D. E., Al-Saadi, J. A.,  
19 Hilton, B. B., Nicks, D. K., Newchurch, M. J., Carr, J. L., Janz, S. J., Andraschko, M. R.,  
20 Arola, A., Baker, B. D., Canova, B. P., Chan Miller, C., Cohen, R. C., Davis, J. E., Dussault,  
21 M. E., Edwards, D. P., Fishman, J., Ghulam, A., González Abad, G., Grutter, M., Herman, J.  
22 R., Houck, J., Jacob, D. J., Joiner, J., Kerridge, B. J., Kim, J., Krotkov, N. A., Lamsal, L., Li,  
23 C., Lindfors, A., Martin, R. V., McElroy, C. T., McLinden, C., Natraj, V., Neil, D. O.,  
24 Nowlan, C. R., O’Sullivan, E. J., Palmer, P. I., Pierce, R. B., Pippin, M. R., Saiz-Lopez, A.,  
25 Spurr, R. J. D., Szykman, J. J., Torres, O., Veefkind, J. P., Veihelmann, B., Wang, H., Wang,  
26 J. and Chance, K.: Tropospheric emissions: Monitoring of pollution (TEMPO), *J. Quant.*  
27 *Spectrosc. Radiat. Transf.*, 186, 17–39, doi:10.1016/j.jqsrt.2016.05.008, 2017.

28  
29

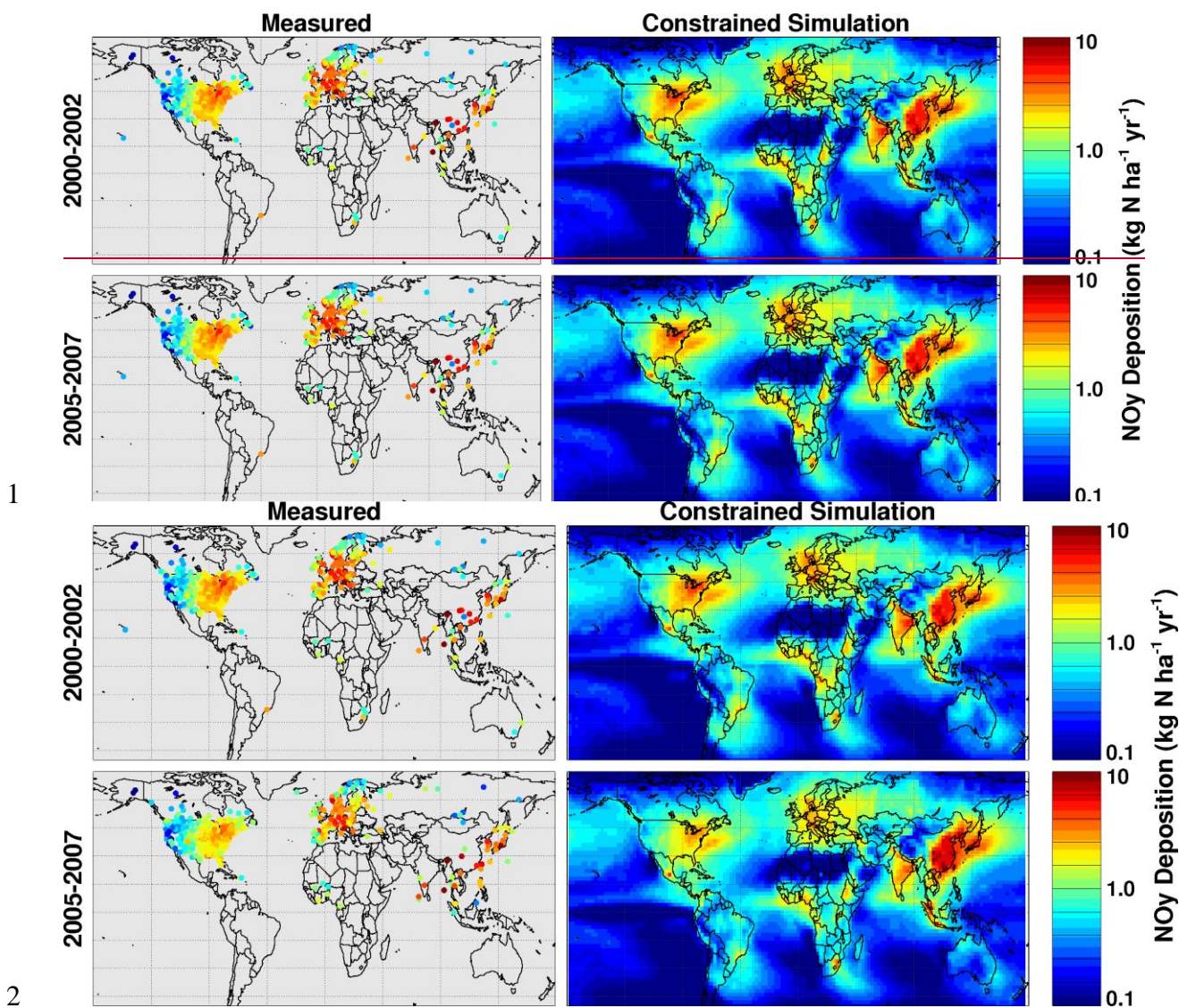
- 1 Table 1: Global top-down NO<sub>x</sub> emissions calculated using the finite mass balance inversion
- 2 approach with observations from GOME, SCIAMACHY, and GOME-2.

<u>Year</u>	<u>Global NO<sub>x</sub> Emissions (Tg N yr<sup>-1</sup>)<sup>a</sup></u>
<u>1996</u>	<u>60.1</u>
<u>1997</u>	<u>58.4</u>
<u>1998</u>	<u>59.2</u>
<u>1999</u>	<u>59.6</u>
<u>2000</u>	<u>53.4</u>
<u>2001</u>	<u>52.3</u>
<u>2002</u>	<u>55.1</u>
<u>2003</u>	<u>50.1</u>
<u>2004</u>	<u>51.5</u>
<u>2005</u>	<u>51.2</u>
<u>2006</u>	<u>50.0</u>
<u>2007</u>	<u>54.7</u>
<u>2008</u>	<u>56.1</u>
<u>2009</u>	<u>55.9</u>
<u>2010</u>	<u>57.5</u>
<u>2011</u>	<u>58.9</u>
<u>2012</u>	<u>59.3</u>
<u>2013</u>	<u>58.5</u>
<u>2014</u>	<u>54.0</u>
<u>Mean</u>	<u>55.6</u>

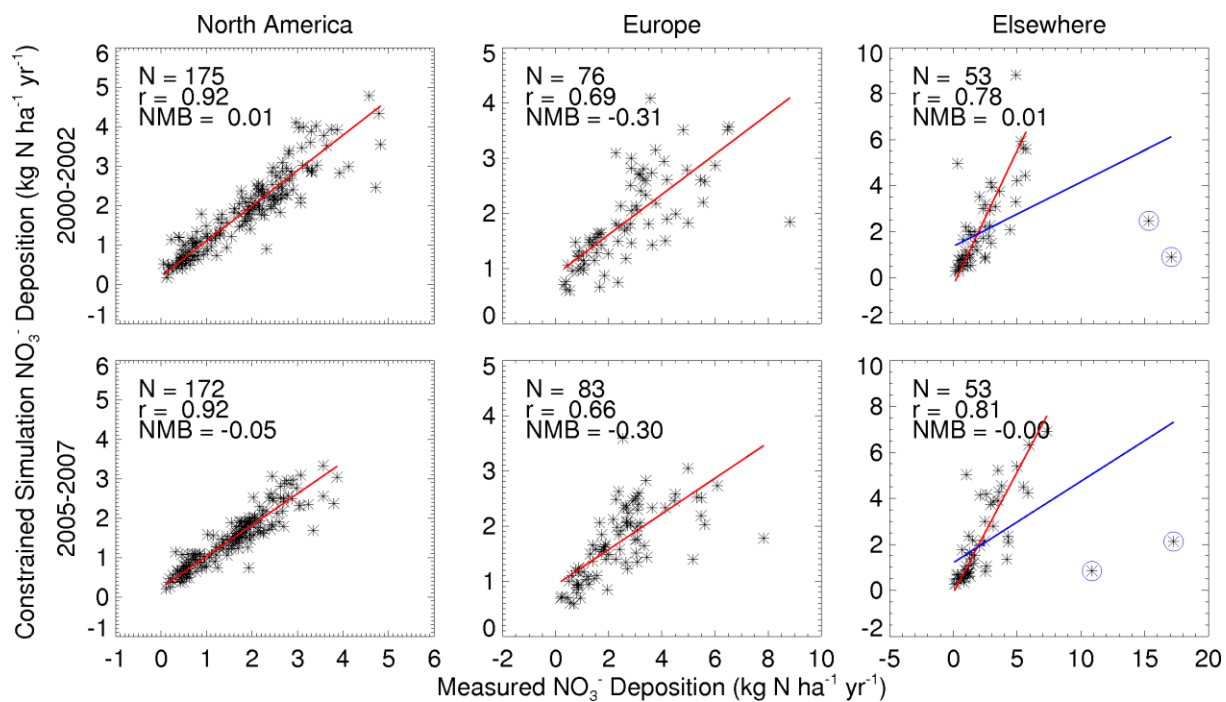
- 3 <sup>a</sup> Includes anthropogenic HNO<sub>3</sub> flux of 2.3 ± 0.1 Tg N yr<sup>-1</sup>.



1  
 2 Figure 1: Long-term (1996-2014) mean  $\text{NO}_y$  deposition derived from the GEOS-Chem  
 3 simulation constrained by satellite observations of  $\text{NO}_2$  columns from the GOME,  
 4 SCIAMACHY, and GOME-2 instruments (top). Mean ratio of simulated dry  $\text{NO}_y$  deposition  
 5 to total  $\text{NO}_y$  deposition (bottom).  
 6

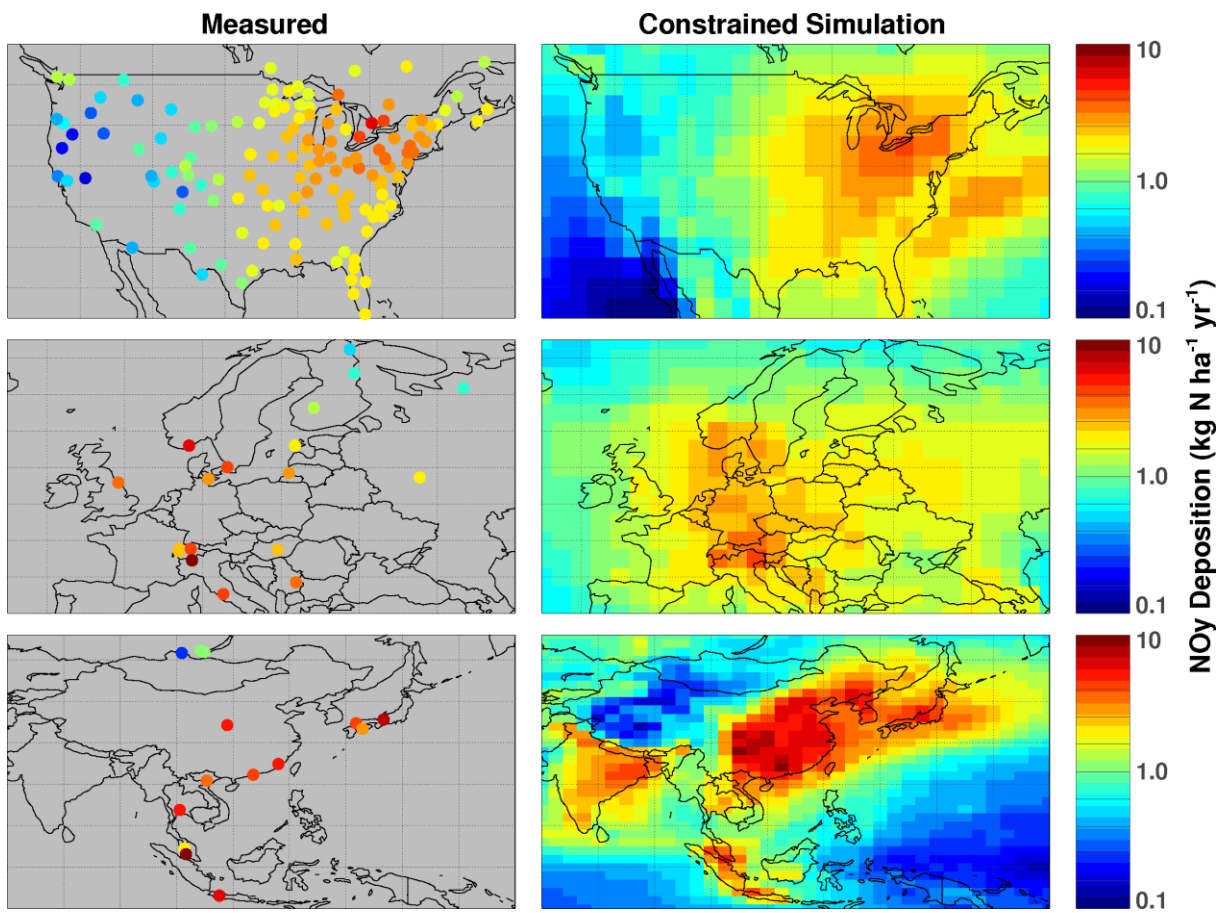


3 Figure 2: Annual wet  $\text{NO}_3^-$  deposition from measurements available through the World Data  
 4 Centre for Precipitation Chemistry, and from the GEOS-Chem simulation constrained with  
 5 satellite observations of  $\text{NO}_2$ . Two time periods are represented: 2000-2002 and 2005-2007.  
 6



1  
 2 Figure 3: Scatter plot of the satellite-constrained simulated wet  $\text{NO}_3^-$  deposition vs.  
 3 measurements available through the World Data Centre for Precipitation Chemistry for  
 4 specific subsets of the data. The red lines show the result of a reduced major axis linear  
 5 regression. In the right column, the blue line shows the fit across all data and the red line  
 6 shows the fit excluding the two circled data points that are discussed in the text (reported  
 7 statistics refer to the red line fit).  
 8

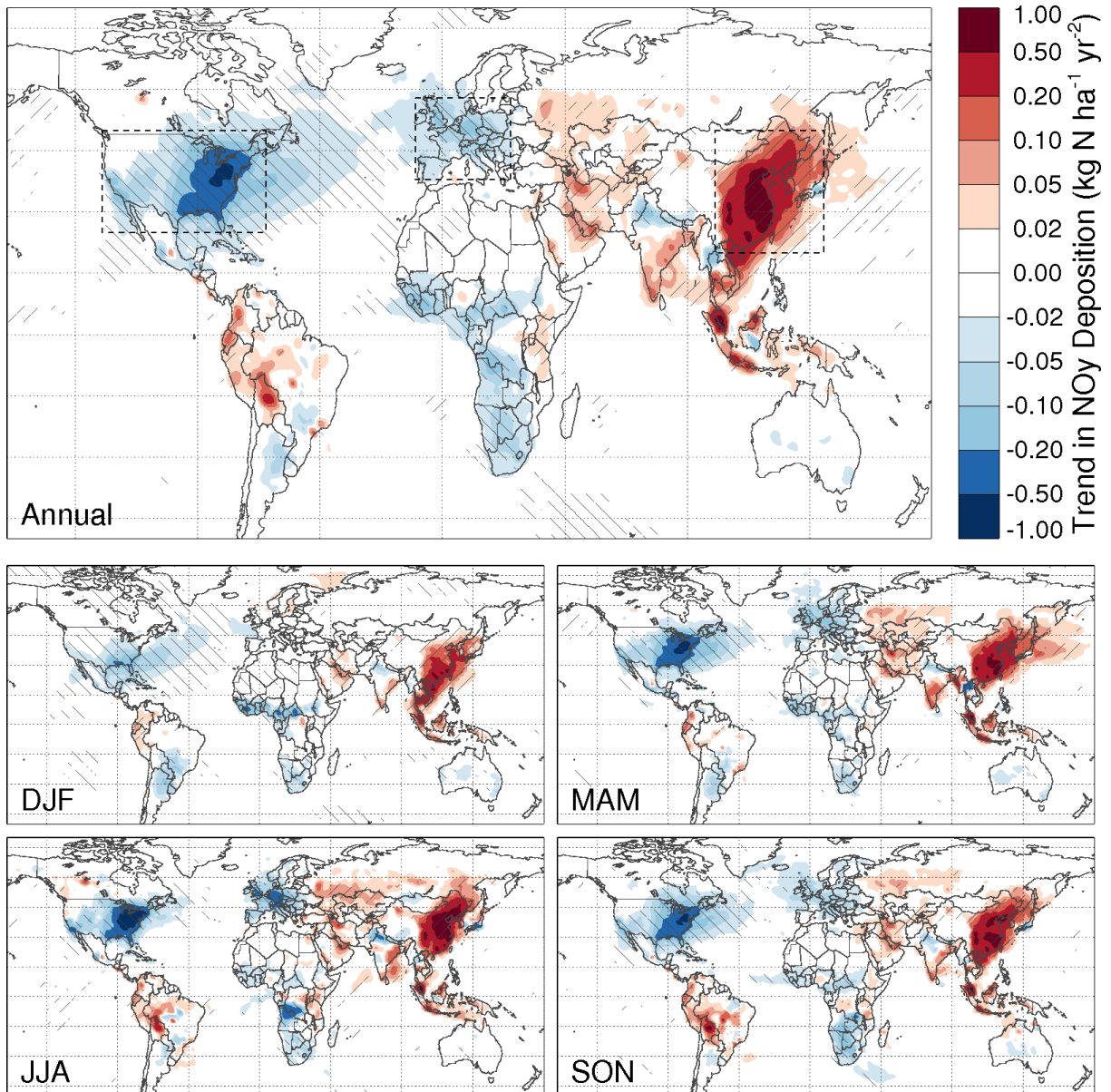




1

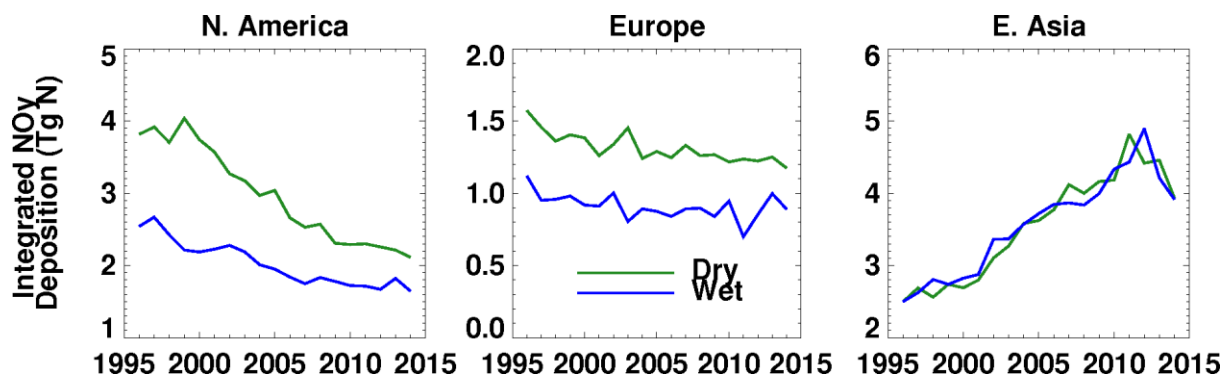
2 Figure 4: Long-term (1996-2014) wet  $\text{NO}_3^-$  deposition from available regional network  
 3 measurements (top: NADP and CAPMON; middle: EMEP; bottom: EANet), and from the  
 4 GEOS-Chem simulation constrained with satellite observations of  $\text{NO}_2$ .

5



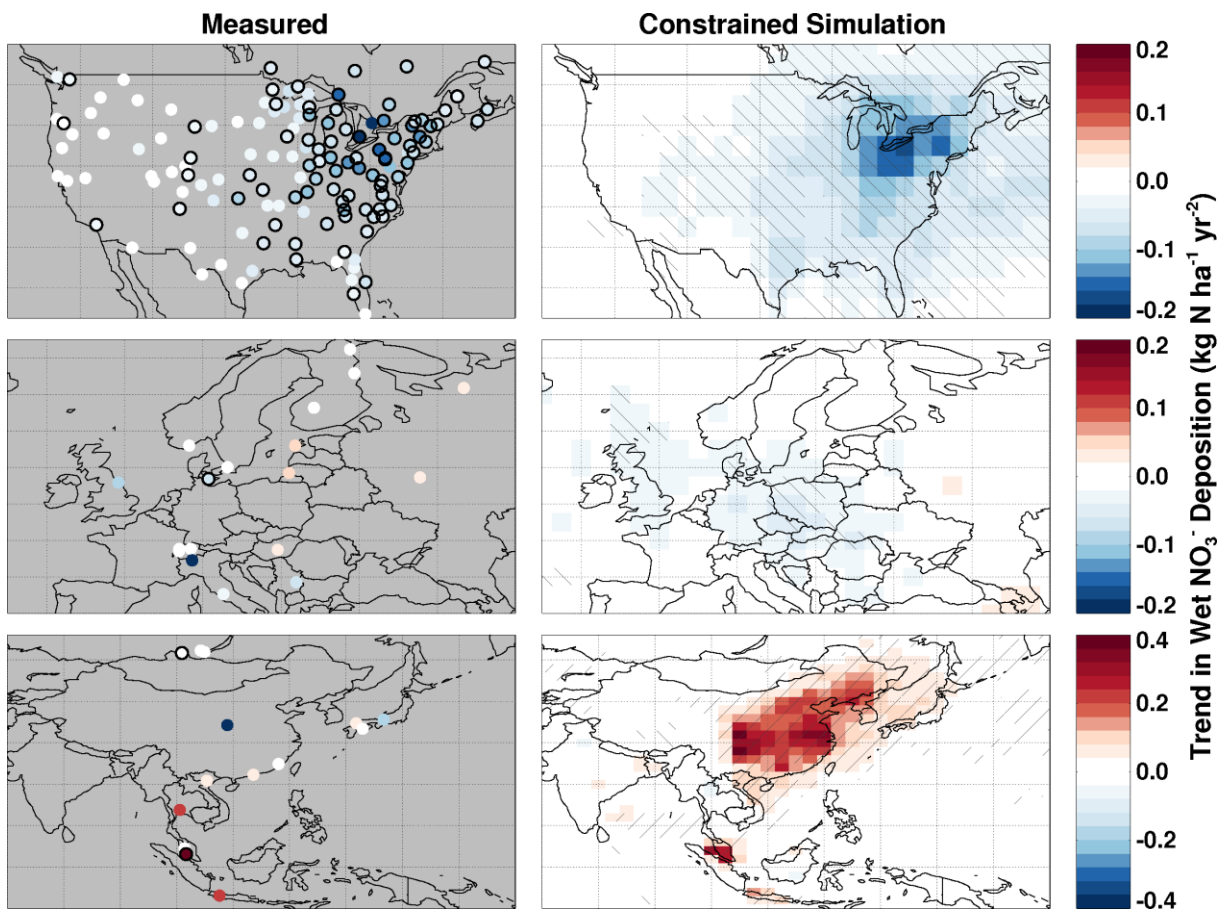
1  
 2 Figure 5. Long-term trend (1996-2014) in the satellite-constrained simulation of NO<sub>y</sub>  
 3 deposition. (A) Annual mean; (B) December-January-February; (C) March-April-May; (D)  
 4 June-July-August; (E) September-October-November. Diagonal hatching represents trend  
 5 significance ( $p < 0.01$ ). Hatching from top-left to bottom-right indicates a decreasing trend;  
 6 hatching from bottom-left to top-right indicates an increasing trend.

7  
 8



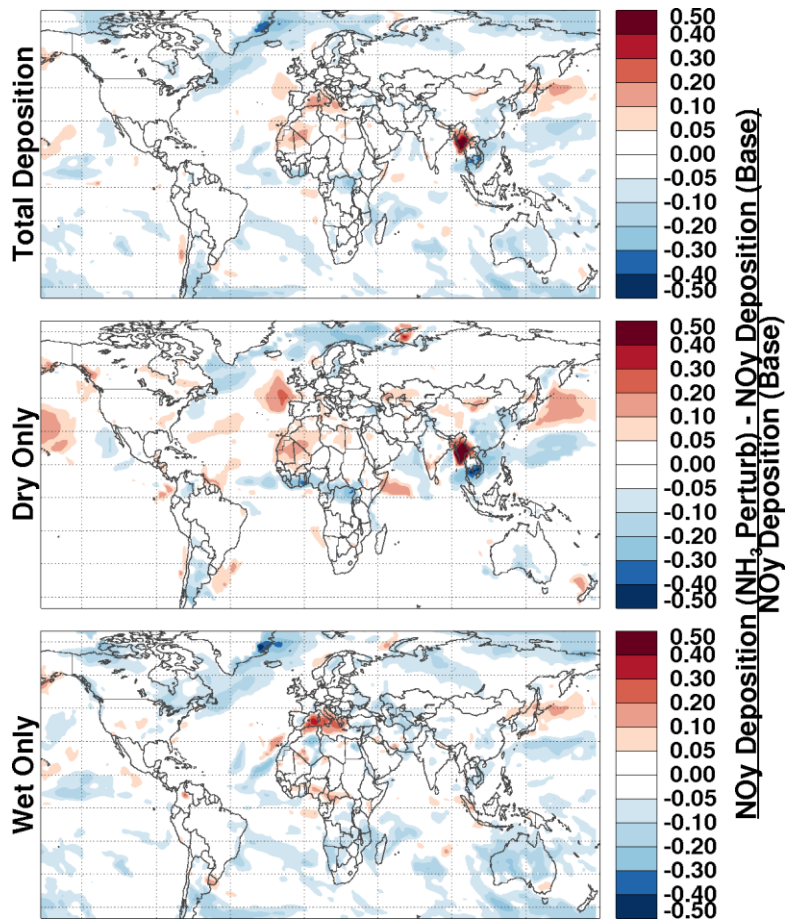
1  
 2 Figure 6: Timeseries of annually integrated dry and wet NO<sub>y</sub> deposition over specific regions  
 3 (North America, Europe, and East Asia) as defined by the dashed rectangles in Figure 5.

4  
 5



1  
 2 Figure 7: Long-term (1996-2014) trends in wet  $\text{NO}_3^-$  deposition from available regional  
 3 network measurements (as in Figure 4), and from the GEOS-Chem simulation constrained by  
 4 satellite observations of  $\text{NO}_2$ . Closed circles around the measurements indicate significant  
 5 trends ( $p < 0.01$ ); hatching indicates statistical significance in the simulation.

6



1  
 2 Figure 8: Sensitivity of simulated NO<sub>y</sub> deposition in 2012 to a 25% perturbation (increase) in  
 3 ammonia emissions in all grid boxes (shown separately for total deposition, dry deposition,  
 4 and wet deposition).